THE JOURNAL OF BIOLOGICAL CHEMISTRY VOL. 289, NO. 50, pp. 34921–34937, December 12, 2014
Published in the U.S.A.

p16 Protein and Gigaxonin Are Associated with the Ubiquitination of NFκB in Cisplatin-induced Senescence of Cancer Cells*

Received for publication, March 26, 2014, and in revised form, October 14, 2014 Published, JBC Papers in Press, October 20, 2014, DOI 10.1074/jbc.M114.568543

Mysore S. Veena[‡], Reason Wilken[‡], Jun-Ying Zheng[‡], Ankur Gholkar[§], Natarajan Venkatesan[‡], Darshni Vira[‡¶], Sameer Ahmed[¶], Saroj K. Basak[‡], Clifton L. Dalgard[‖], Sandhiya Ravichandran[‡], Raj K. Batra[‡‡§§], Noriyuki Kasahara[‡‡], David Elashoff[‡‡], Michael C. Fishbein[¶¶], Julian P. Whitelegge[‖‖], Jorge Z. Torres[§ §§], Marilene B. Wang[‡¶§§], and Eri S. Srivatsan[‡§§1]**

From the [‡]Department of Surgery, Veterans Affairs Greater Los Angeles Healthcare System/David Geffen School of Medicine at UCLA, Los Angeles, California 90073, [§]Department of Chemistry and Biochemistry, UCLA, Los Angeles, California 90095, [¶]Department of Head and Neck Surgery, David Geffen School of Medicine at University of California Los Angeles, Los Angeles, California 90095, [‖]Departments of Anatomy, Physiology, and Genetics, Uniformed Services University, Bethesda, Maryland 20814, [**]Division of Pulmonary and Critical Care Medicine, Department of Medicine, Veterans Affairs Greater Los Angeles Healthcare System, Los Angeles, California 90073, [‡‡]Department of Medicine and [¶¶]Pathology and Laboratory Medicine, David Geffen School of Medicine at University of California Los Angeles, Los Angeles, California, [‖‖]Department of Psychiatry and Biobehavioral Sciences, UCLA, Los Angeles, California 90095, and [§§]Jonsson Comprehensive Cancer Center, UCLA, Los Angeles, California 90095

Background: Molecular mechanism of p16-mediated cellular senescence in cisplatin-treated cells is not known.
Results: Cisplatin treatment leads to p16 nuclear transport and association with gigaxonin for the ubiquitination of NFκB.
Conclusion: A protein associated with neural diseases is involved in cisplatin-mediated cellular senescence.
Significance: Nuclear expression of p16 and gigaxonin is a useful marker of cancer cell chemosensitivity.

The molecular mechanism of p16-mediated senescence in cisplatin-treated cancer cells is not fully understood. Here we show that cisplatin treatment of head and neck cancer cells results in nuclear transport of p16 leading to a molecular modification of NFκB. Chromatin immunoprecipitation assays show that this modification is associated with the inhibition of NFκB interacting with its DNA binding sequences, leading to decreased expression of NFκB-transcribed proteins. LCMS proteomic analysis of LAP-TAP-purified proteins from HeLa cells containing a tetracycline-inducible GFP-S peptide-NFκB expression system identified gigaxonin, an ubiquitin E3 ligase adaptor, as an NFκB-interacting protein. Immunoblotting and siRNA studies confirmed the NFκB-gigaxonin interaction and the dependence of this binding on p16-NFκB binding. Using gel shift assays, we have confirmed p16-NFκB and gigaxonin-NFκB interactions. Furthermore, we have observed increased NFκB ubiquitination with cisplatin treatment that is abolished in the absence of p16 and gigaxonin expression. Analysis of 103 primary tumors has shown that increased nuclear p16 expression correlates with enhanced survival of head and neck cancer patients ($p < 0.0000542$), indicating the importance of nuclear p16 expression in prognosis. Finally, p16 expression is associated with reduced cytokine expression and the presence of human papilloma virus in chemoradiation-sensitive basaloid tumors. However, the absence of p16 expression is associated with enhanced cytokine expression and the absence of human papilloma virus in aggressive tumors. These results clearly demonstrate that nuclear p16 and gigaxonin play an important role in chemosensitivity of head and neck cancers through ubiquitination of NFκB.

Head and neck squamous cell carcinoma (HNSCC)[2] is the sixth most common form of cancer worldwide and represents ~5% of all cancers diagnosed annually in the United States (1, 2). Every year >42,000 cases of oral, laryngeal, and pharyngeal cancer are diagnosed and >12,000 individuals die of the disease (3). The diagnosis and treatment of head and neck cancer presents several unique challenges. By virtue of their inconspicuous location, many cases of HNSCC are not discovered until the cancer is at a later stage, not uncommonly until after spread to lymph nodes in the neck. Early stage tumors may be treated primarily with surgery or radiotherapy, but more advanced cancers often require multimodality therapy with surgery, radiation, and chemotherapy, which can result in very high morbidity (4).

Platinum-based agents form the backbone of the standard chemotherapeutic regimens for head and neck cancer. Cisplatin (*cis*-diamminedichloroplatinum) is a widely used drug in the class of platinum-based chemotherapies, and the adverse

* This work was supported, in whole or in part, by National Institutes of Health Grant R21 CA116826-01 (to M. W.). This work was also supported by a merit grant from Veterans Affairs, Washington, D. C. (to E. S. S.), by funds from Veterans Affairs Greater Los Angeles Healthcare System, West Los Angeles Surgical Education Research Center, and by a UCLA Academic Senate grant (to M. W.).

[1] To whom correspondence should be addressed: Dept. of Surgery, VAGLAHS/David Geffen School of Medicine at UCLA, Bldg. 304, Rm. E2-218, 11301 Wilshire Blvd., Los Angeles, CA 90073. Tel.: 310-268-3217; Fax: 310-268-3190; E-mail: esrivats@ucla.edu.

[2] The abbreviations used are: HNSCC, head and neck squamous cell carcinoma; MTT, 3-(4,5-dimethylthiazol-2-yl)-2,5-diphenyltetrazolium bromide; HPV, human papilloma virus 16; TEV, tobacco etch virus; CSC, cancer stem cell; GALV, gibbon ape leukemia virus; CDDP, cisplatin; Rb retinoblastoma; EGFR, EGF receptor; LAP-TAP, localization and affinity purification (LAP = EGFP-TEV-S-peptide)-tandem affinity purification; ALDH-1, aldehyde dehydrogenase 1; BMI-1, B cell specific Moloney murine leukemia virus integration site-1.

effects of cisplatin are significant and include renal toxicity, nerve damage, hearing loss, and bone marrow suppression (5). The efficacy of cisplatin in HNSCC is greatly increased when combined with other chemotherapeutic agents, such as taxanes (paclitaxel and docetaxel) and 5-fluorouracil (5, 6). The precise molecular mechanism of cisplatin is unknown, but there is evidence that cisplatin may work through a p16- and p53-dependent mechanism (7). p16 and p53 are both tumor suppressor genes that function in cell cycle regulation, and mutations of these genes are linked to cancer development. Data suggest that cisplatin inhibits HNSCC growth through p16-mediated cell cycle arrest, and decreased expression of p16 has been linked to cisplatin resistance (7).

NFκB is an inducible transcription factor that regulates the expression of genes involved in inflammation as well as the control of cell proliferation and survival (8–10). NFκB is a heterodimeric protein and is retained in the cytoplasm in an inactive form by IκB (inhibitor of NF-κB), which is composed of α and β subunits. Upon receipt of the appropriate chemical signals such as TNF-α that initiate NF-κB activation, several steps are required to free NF-κB from this inhibitory binding. IκB must be phosphorylated at its α subunit by IκK (inhibitor κ B kinase, composed of α, β, and γ subunits), which results in ubiquitination and degradation of the phosphorylated IκBα and the release of NF-κB from its stationary location in the cytoplasm. The unbound NF-κB is then transported to the nucleus where it could bind to DNA and activate transcription.

NFκB is involved in cellular responses to stressful stimuli such as cytokines, UV irradiation, free radicals (including cigarette smoke), hypoxia, and infectious agents (11, 12). Activation of NFκB is increased in many cancers and is associated with various steps in the development of malignancy such as expression of anti-apoptotic genes, angiogenesis, tumor promotion, and metastasis (9). A variety of cancers, including HNSCC, have demonstrated constitutive expression of NFκB (13–15). As a result, modulation of NFκB has emerged as a potential therapeutic target in anti-cancer research. Here we show that cisplatin treatment leads to nuclear transport of p16, resulting in the recruitment of gigaxonin for the ubiquitination of NFκB.

EXPERIMENTAL PROCEDURES

Primary Tumor samples—Primary HNSCC tumors were obtained from the UCLA Medical Center and the cooperative human tissue network of the National Institutes of Health. Human tissues were obtained after the approval from the Institutional Review Board committees of the West Los Angeles VA Medical Center and UCLA. A total of 116 tumors were analyzed. Immunohistochemistry was performed on 103 tumors. Thirteen tumors and two normal tissues were used for Western blot analysis.

HNSCC Cell Lines—The HNSCC cell lines CCL23, CAL27, UM-SCC1, and UM-SCC14A representing laryngeal, tongue, and oral cavity carcinomas were used. Although CCL23 and CAL27 cell lines were obtained from the American Type Culture Collection, cell lines UM-SCC1 and UM-SCC14A were obtained from Dr. Thomas E. Carey (University of Michigan, Ann Arbor, MI). MTT growth viability assays were carried out using the established protocol.

β-Galactosidase Senescence Assay—CCL23 cells grown to 50–60% confluence in 6-well plates were treated with cisplatin (6 μg/ml) for 4 h and then in fresh medium for 72 h. Untreated and treated cells were stained for β-galactosidase using the standard protocol.

Vector Construct—Well characterized 390 amino acid-NFκB cDNA (Clontech) was amplified and cloned into pDONR221 using the Gateway BP Clonase II (Invitrogen) and subsequently into pGLAP1 N-term EGFP-TEV-S tag vector using the Gateway LR Clonase II (Invitrogen) as previously described (16). Stable cell lines were generated by transfecting HeLa Flp-In T-REx cells with pGLAP1-NFκB vector, using FuGENE 6 transfection reagent (Promega Scientific). Positive clones were selected by treating cells with 400 μg/ml hygromycin B and checked for protein expression with 0.2 μg/ml doxycycline (16).

Cisplatin Treatment—Stable cell lines expressing NFκB were plated in serum-free media for 24 h and treated with complete media containing 3 or 6 μg of cisplatin or no cisplatin along with 0.2 μg/ml doxycycline and treated for 4 h. Post-treatment the cells were washed 3 times with PBS and further grown for 24 h in complete medium containing 0.2 μg/ml doxycycline.

Immunoprecipitation—Cytoplasmic and nuclear protein extracts were prepared with the cisplatin-treated and non-treated NFκB cell lines using the Subcellular Protein Fractionation kit (Thermo Scientific). Protein concentrations in the lysates (nuclear/cytoplasmic extracts) were determined by the nanodrop method at an absorbance 280, and the lysates were accordingly diluted with respective buffers to have equal protein concentrations. Although 20 μg of lysates were used as inputs, 100 μg of the lysates were used for the immunoprecipitation studies.

PCR of the p16 Gene—DNA (500 ng) isolated from SiHa (human papilloma virus 16 (HPV 16)-containing cervical cancer cell line), CCL23, CAL27, and UM-SCC1 cell lines were used for the PCR using a prior denaturation at 95 °C for 5 min. PCR conditions used included denaturation at 94 °C for 30 s, a step down annealing for 30 s, and extension at 72 °C for 45 s with a final extension at 72 °C for 7 min. A step-down annealing temperature of 60 °C to 57 °C for 5 cycles, each followed by 15 cycles at 56 °C for exon 1, and a step-down annealing temperature of 57 °C to 53 °C for 3 cycles, each followed by 19 cycles at 52 °C for exon 2, were used. Primers exon 1 forward 5′ GAA GAA AGA GGA GGG GCT GG 3′, exon 1 reverse 5′ GCG CTA CCT GAT TCC CAA TTC 3′, exon 2 forward 5′ TGG CTC TGA CCA TTC TGT TC 3′, and exon 2 reverse 5′ TTT GGA AGC TCT CAG GGT AC 3′ were used. PCR products of 340 and 382 bp for exons 1 and 2, respectively, were verified on 10% polyacrylamide gels. Sequencing was performed using Sanger sequencing protocol in the Nextgen sequencer (Invitrogen), and the sequences were compared with the NCBI blast database.

Quantitative RT-PCR for CD44—Total RNA was isolated using the RNeasy Mini Kit (Qiagen, Valencia, CA), and concentration was determined by spectrophotometry. Reverse transcription of 1.0 μg of total RNA was completed using the iScript cDNA Synthesis kit (Bio-Rad). Quantitative PCR was performed on a CFX384 Real-Time PCR Detection System (Bio-

Rad) using SsoFast EvaGreen Supermix (Bio-Rad) with 300 nM primer concentration and an ~5-ng cDNA input. Raw Ct values were calculated as an average of four technical replicates. Relative gene expression values were calculated after normalizing to the values of the housekeeping gene LDHA (lactate dehydrogenase A) and relative to control samples. Primers used were CD44 forward 5′-CCC AGA TGG AGA AAG CTC TG-3′, CD44 reverse 5′-GTT GTT TGC TGC ACA GAT GG-3′, lactate dehydrogenase A forward 5′-CTG CCA CCT CTG ACG CAC CA-3′, and lactate dehydrogenase A reverse-5′ AAA CAT CCA CCT GGC TCA AGG GG-3′.

Western Blot Analysis—Twenty μg of protein and prestained protein markers were subjected to SDS-PAGE in 10% gels under reducing conditions, and proteins were electrotransferred to polyvinylidene difluoride membranes (Millipore, Inc.). In the case of LAP-TAP-purified samples, the immunoprecipitated and unbound samples were resolved in 4–20% Tris-glycine SDS gels followed by Western transfer and hybridization of proteins in blots to anti-NFκB, anti-p16, anti-cyclin D1, anti-CDK4 (Santa Cruz Biotechnology), anti-gigaxonin (Sigma), anti-histone H3 (Abcam Biotechnologies), anti-GAPDH (GeneTex), and anti-comm D1 (gift of Dr. Ezra Burstein) antibodies. After hybridization with the secondary antibody, membranes were developed as described (17).

Purification and LCMS—The NFκB cell line was cultured and induced with 0.2 μg/ml doxycycline for 24 h, post with or without cisplatin treatment. The cells were lysed, and the lysate was subjected to LAP-TAP purification (16). Briefly, NFκB was immunoprecipitated by incubating the protein extracts with GFP antibody-coupled protein-A beads. After incubation, unbound supernatant was removed, and the beads with GFP-bound proteins were thoroughly washed. Proteins were then eluted by boiling the beads with reducing sample buffer. The solubilized proteins were treated with TEV enzyme and then precipitated with S-tag peptide. The beads containing S-tag pulldown proteins were again washed, and the bound proteins were solubilized by boiling with reducing sample buffer. This double immunoprecipitation method improves specificity of NFκB-bound proteins. The eluted samples were resolved on 4–20% Tris-glycine SDS gels and cut into slices that were then digested with trypsin for LCMS analysis. The proteomic MASCOT program was used to identify proteins with and without modification settings. For the control, p16 or gigaxonin siRNAs transfections, cells at 70% confluence were transfected with the siRNA in the Opti-MEM media (Invitrogen). Twelve hours later minimum Eagle's medium was added, and 48 h later protein lysates were collected for the immunoblot analysis.

Gel Shift Assay—Gel shift assays were carried out as described (18). Oligonucleotides representing the consensus NFκB binding site were used in the assay. An NF-κB oligonucleotide sequence containing a mutation at the binding site and oligonucleotide sequences representing the activator protein 1 binding site were used as controls. For supershift assays, the lysates were incubated with anti-EGFR (U. S. Biologicals), anti-p16, anti-p21 (Santa Cruz Biotechnology), or anti-gigaxonin (Sigma) antibody for 15 min at room temperature before the addition of the labeled oligonucleotide.

Ubiquitination Assay—HeLa or CCL23 cells were grown in minimum Eagle's medium to 75% confluence and treated with cisplatin (6 μg/ml) for 4 h. Cisplatin-free media was added, and the cells were incubated for 20 h. Cells were then treated with protease inhibitor (MG-132, 10 μM) and deubiquitinase inhibitor (*N*-ethylmaleimide, 10 μM) for 4 h, and the lysates were prepared in the ice bath by incubation with the lysis buffer (50 mM HEPES, 200 mM KCl, 1 mM EGTA, 1 mM $MgCl_2$, 0.5 mM DTT, 0.5% Nonidet P-40 containing protease and phosphatase inhibitors) for 15 min. The lysate was spun at 15,000 rpm for 10 min, and the supernatants were used for protein concentration measurements and immunoblot analysis. Proteins were immunoprecipitated with anti-NFκB antibody (Santa Cruz Biotechnology) and hybridized to the control IgG or multiplex hybridization to NFκB and anti-ubiquitin antibodies (BML-PW8810-0100, Enzo Life Sciences). After secondary antibody (IR680 and IR800; Li COR, Corp.) hybridization, membranes were developed as described (17). For the siRNA studies, cisplatin treatment was initiated 24 h after siRNA transfections.

Chromatin Immunoprecipitation (ChIP) Assay—Chromatin immunoprecipitation assays were performed using the assay kit (17). Immunoprecipitations were carried out using NFκB (Calbiochem) and IgG (Santa Cruz Biotechnology, Santa Cruz, CA) antibodies. DNA isolated from the input as well as the immunoprecipitated samples were amplified using IL-8 and β-actin primers. PCR products were separated on 10% polyacrylamide gels and stained with ethidium bromide, and images were captured using the Kodak Gel documentation system.

Immunofluorescence—Cells grown to 50–60% confluence were subjected to cisplatin treatment, and immunofluorescence was performed as described (7).

Immunohistochemistry—Paraffin sections (5 μm) of tumor samples were dewaxed and hybridized to p16 antibody after standard immunohistochemical protocol (19). Two pathologists were involved in independent scoring of hybridization intensities. The percentage expression was calculated with respect to the total number of cells present in the slide. Intensity was determined 1+ to 4+ as minimum to maximum intensity respectively. At least two slides were evaluated for most of the samples.

Statistical Analysis—The *p* values for the MTT growth assays were calculated using Student's *t* test at 95% confidence interval. Results are presented as the means ± S.D. For the quantitative RT-PCR, statistical analysis for differential expression was performed by one-way analysis of variance with multiple pairwise comparisons with Sidak correction. The log-rank test and Cox proportional hazards regression analysis was used to assess the relationship of nuclear p16 expression to overall survival.

RESULTS

Nuclear p16 Expression Correlates with Cisplatin Sensitivity in HNSCC Cell Lines—Cell growth assays showed CCL23 and CAL27 to be sensitive to cisplatin treatment, UM-SCC14A to be intermediately sensitive, and UM-SCC1 to be resistant (Fig. 1*A*). Immunofluorescence studies demonstrated base-line cytoplasmic and nuclear p16 expression in untreated CCL23

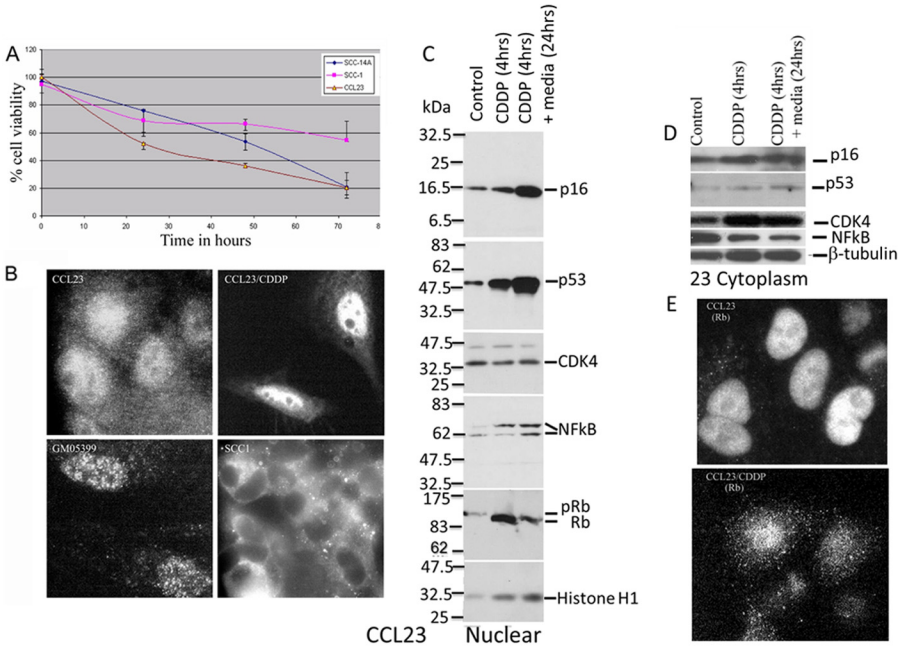

FIGURE 1. **Nuclear p16 expression correlates with cisplatin sensitivity in HNSCC cell lines.** *A*, comparative sensitivity of HNSCC cell lines to cisplatin (CDDP). Treatment with CDDP (6 μg/ml) for 4 h followed by growth in drug-free medium shows CCL23 to be sensitive and UM-SCC1 to be resistant. *B*, immunofluorescence staining for p16 shows nuclear p16 expression in CCL23 cells, and the intensity increases after treatment with CDDP. However, p16 expression remains largely cytoplasmic in UM-SCC1 cells. A fibroblast cell line with low level nuclear expression is also shown for comparison. *C*, Western blot studies confirm an increase in the level of nuclear p16 and p53 expression after treatment with CDDP for 4 h and in cells grown in drug-free medium for a further 24 h. The level of phospho-Rb expression is also reduced in CCL23 cells after CDDP treatment. The nuclear NFκB shows a higher molecular weight band after treatment with CDDP. *D*, there is very little difference in the expression of p16, p53, and NFκB in the cytoplasmic fraction of treated samples. *E*, immunofluorescence with phospho-Rb antibody confirms degradation of the phospho Rb protein in CDDP-treated CCL23 cells. Immunofluorescence pictures in *B* and *E* represent 100× magnification.

cells (Fig. 1*B*). After cisplatin treatment, p16 localization shifted to the nucleus. In contrast, immunofluorescence studies in UM-SCC1 cells showed p16 localization to the cytoplasm (Fig. 1*B*). No shift to nuclear p16 localization was observed after cisplatin treatment (data not shown). The presence of increased nuclear p16 expression in CCL23 cells after cisplatin treatment was confirmed by Western blot analysis of both nuclear and cytoplasmic cell extracts (Fig. 1, *C* and *D*). Increased p16 expression was accompanied by a molecular modification, the appearance of a higher molecular weight band, in NFκB of the nuclear extract (Fig. 1*C*). This shift was not seen in the cytoplasmic extract (Fig. 1*D*). The retinoblastoma protein (pRb) is the product of the Rb tumor suppressor gene and is also an important regulatory molecule controlling entry into the cell cycle. Phosphorylation of Rb is associated with release of the transcription factor E2F and increased transcription of genes involved in cell division (20, 21). In addition to increased nuclear expression of p53, decreased nuclear phospho-Rb expression was also seen in the cisplatin-treated CCL23 cell extracts (Fig. 1*C*). Immunofluorescence studies of CCL23 cells treated with cisplatin also demonstrated reduced phosphorylation of Rb (Fig. 1*E*).

Increased p16 Expression Correlates with Decreased Cyclin D1 Expression—Western blot analysis of the different HNSCC cell lines has demonstrated that CCL23 expresses p16, whereas p16 expression was reduced or absent in the other HNSCC cell lines (Fig. 2*A*). Although CAL27 cells were sensitive to cisplatin treatment, p16 expression was not seen. Therefore, we investigated the genomic status of the p16 gene. PCR analysis followed by sequencing of the two exons showed nonsense mutation at codon 69, resulting in the conversion of glutamic acid to a stop codon (E69*, GAG205UAG). We could not detect a shorter p16 protein in the Western blots possibly due to degradation. In CAL27 cells we have attributed cisplatin sensitivity to the nuclear expression of p53 (7). Analysis of cyclin D1 expression showed an inverse relationship to p16 expression, with CCL23 expressing low levels of Cyclin D1 and the other cell lines demonstrating high levels of Cyclin D1 (Fig. 2*B*). Treatment of cisplatin-sensitive cell lines, CCL23 and CAL27, showed decreased expression of cyclin D1 upon cisplatin treatment (Fig. 2*C*). Cyclin D1 levels were not altered in the resistant cell lines UM-SCC1 and UM-SCC12 (Fig. 2*D*).

Increased Cancer Stem Cell (CSC) Marker, CD44, Expression Correlates to Cisplatin Resistance—Cisplatin resistance has also been shown to be related to the formation of CSCs. Therefore, we investigated the expression of the CSC marker CD44 in CCL23 and UM-SCC1 cells. Expression of CD44 was 5-fold higher in UM-SCC1 cells in comparison with that of CCL23 cells (Fig. 2*E*). CCL23 cells selected in 8 μg/ml cisplatin showed a 2.5-fold increased expression, confirming an increase in CSCs after cisplatin treatment. Increase in CD44 expression was minimal in UM-SCC1 cells selected in 3 μg/ml cisplatin. Additionally, our earlier studies have also shown increased secretion of cytokines IL-6 and IL-8 in the resistant cell lines, indicating increased presence of CSCs in the resistant cell lines (Table 1). These studies, therefore, indicated an increased NFκB transcription activity in cisplatin-resistant cells.

Mobility Shift of NFκB Complex after Cisplatin Treatment—It has been established that cisplatin treatment leads to senescence through the activation of p16 and p21 proteins. However,

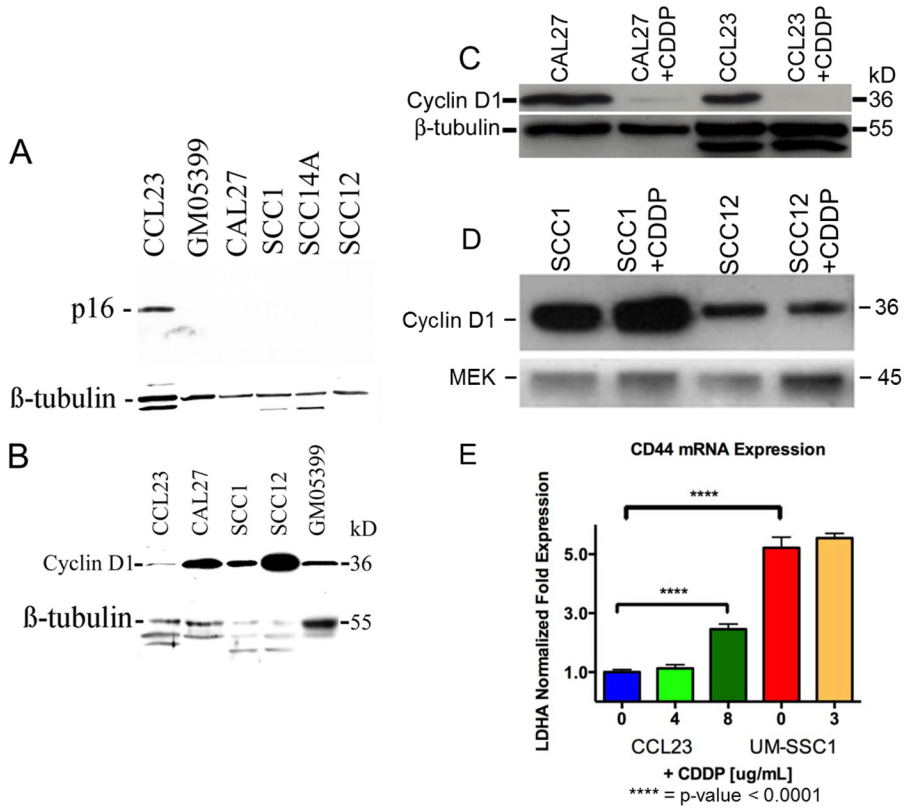

FIGURE 2. **Inverse relationship between p16 and cyclin D1 expression and CD44 expression in HNSCC cell lines.** *A*, Western blot analysis demonstrates p16 expression in extracts of CCL23 cells but not in CAL27, UM-SCC1, or UM-SCC14A cell lines. *B*, cyclin D1 expression is reduced in CCL23 cells expressing p16, whereas the p16-deficient cell lines CAL27, UM-SCC1, UM-SCC12, and UM-SCC14A demonstrate higher levels of cyclin D1 expression. Cisplatin treatment of CCL23 and CAL27 cell lines leads to reduction in the expression of cyclin D1 (*C*); however, cisplatin treatment does not affect the expression of cyclin D1 in resistant cell lines UM-SCC1 and UM-SCC12 confirming the inverse relationship between cyclin D1 and p16 in CCL23 and p53 in both CCL23 and CAL27 cell lines (*D*). *E*, CD44, a marker of CSCs is 5-fold higher in the resistant UM-SCC1 cells in comparison to CC23 cells. Although selection with cisplatin does not affect CD44 expression in the resistant cell line, there is a 2.5-fold increase in CD44 expression in CCL23 cells grown in 8 μg/ml cisplatin. Thus, cisplatin resistance seems to be related to the development of CSCs.

TABLE 1

Cisplatin sensitivity and the expression of cell cycle and cytokine genes in HNSCC cell lines

ND, not done; IF, immunofluorescence data; Cyt, cytoplasm; Nuc, nucleus.

		p16 expression					p53 expression						
				IF					IF				
Cell line	Cisplatin sensitivity[a]	Status (PCR data)	Western	Cyt	Nuc	Cyclin D1 expression Western[b]	Status (PCR data)	Western[b]	Cyt	Nuc	Rb Status[c]	IL-6 expression[d]	IL-8 expression[d]
CCL23[e]	Most sensitive	Wild	+	+	+	1	Wild	3	+	+	Wild	85	95
CAL27[f]	Sensitive	Mutant[g]	0	−	−	3	Mutant[h]	5	+	+	Wild	300	300
UM-SCC1	Least sensitive	Wild	0	+	−	2	Wild/mutant[i]	2	+	−	Wild	475	2000
UM-SCC14A	Less sensitive	ND	0	−	−	4	Mutant[γ]	1	+	−	Wild	600	450

[a] In relationship to the sensitivity of CCL23 cells.
[b] Western blot intensity measured as 1 being the lowest and 5 being the highest expression.
[c] Inferred from the presence of hypo and hyper phosphorylated forms of the Rb protein.
[d] Expression level in the cell supernatant (pg/ml) measured by the ELISA assay (59).
[e] HPV 18-containing cell line. All other cell lines are HPV negative.
[f] p53 expression in CAL 27 cells (7).
[g] Nonsense exon 2 mutation in codon 69 resulting in the conversion of glutamic acid to a stop codon (E69*, GAG205UAG); present investigation.
[h] Missense exon 6 mutation in codon 193 resulting in the conversion of histidine to a leucine (H193L, CAC578CUC) (7).
[i] Exon 3 and exon 8 skipping in UM-SCC1 and UM-SCC14A cell lines respectively (24).

the molecular mechanism is not known. As expected, cisplatin treatment led to the expression of senescence marker β-galactosidase around the nucleus in CCL23 cells confirming cisplatin sensitivity (Fig. 3*A*). Because there is an indication in the literature for the association of exogenously expressed p16 and NFκB (22), we wanted to determine whether an *in vivo* association also exists between p16 and NF-κB. A gel mobility shift assay was performed using the lysates collected from control (untreated) and cisplatin-treated CCL23 cells and the consensus NFκB binding site oligonucleotide probe. The presence of a band with CCL23 lysate indicated the binding of the oligo probe to the NFκB complex (Fig. 3*B*). Reduced intensity of this band with the inclusion of the cold oligonucleotide and not with cold mutant oligonucleotide or a nonspecific activator protein 1 binding site oligonucleotide confirmed the specificity of binding to NFκB. Treatment of CCL23 cells with cisplatin for 8 h showed a shift of NFκB-bound oligonucleotide to a higher molecular weight band. A near complete shifting to the higher

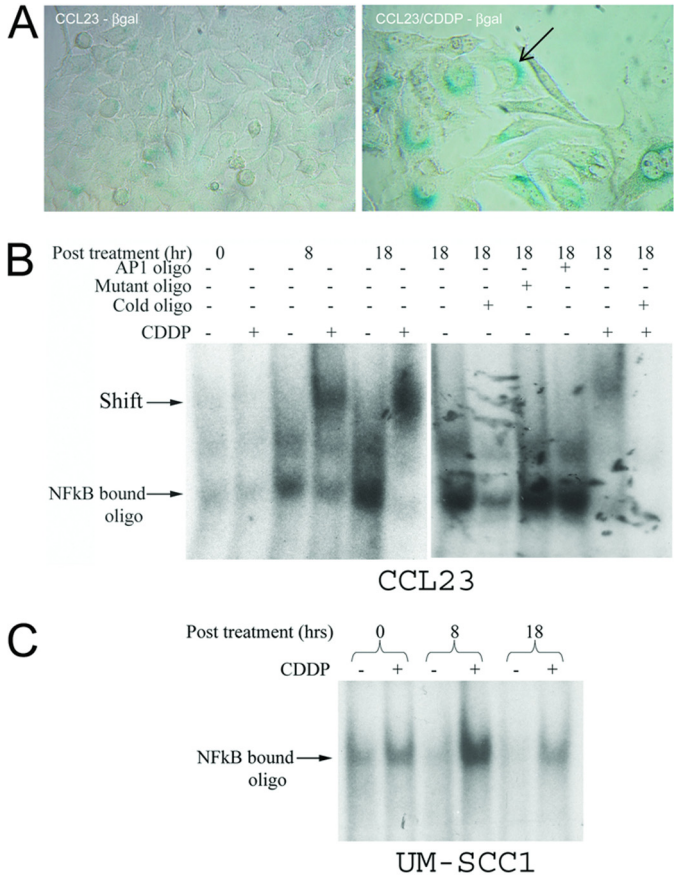

FIGURE 3. **Cisplatin-induced senescence in CCL23 cells involves a mobility shift of the NFκB complex.** *A*, untreated and CDDP-treated cells were stained with the senescence marker β-galactosidase. The blue staining around the nucleus is clearly visualized in CDDP-treated cells (the *arrow* points to one of these stained cells) indicating cellular senescence. The proliferating control cells show only a faint background blue staining. Pictures represent 100× magnification. *B*, gel shift assay using ^{32}P-labeled NFκB oligonucleotide shows NFκB-bound oligo probe in untreated CCL23 cells, more visible in cells grown for 18 h. This binding is abolished with the inclusion of the cold oligo probe and not in the presence of a mutant or a nonspecific activator protein 1 oligonucleotide. A mobility shift to a higher molecular weight region of the NFκB-oligo probe complex is seen in CDDP-treated cells. The shift (more prominent post 18 h CDDP treatment) represents binding of additional proteins to the DNA-bound NFκB. Again, this binding is abolished with the cold oligonucleotide confirming the specificity of the complex. *C*, mobility shift of the NFκB-bound oligo probe is not observed in resistant UM-SCC1 cells treated with CDDP, indicating the absence of additional protein binding to NFκB.

molecular weight band was seen with an 18-h cisplatin treatment. This mobility shift was abolished with the inclusion of cold NFκB oligo confirming the specificity of this protein-DNA binding. The mobility shift of NFκB-bound oligonucleotide was not seen with the lysate from the untreated or cisplatin-treated UM-SCC1 cells (Fig. 3*C*). Thus, our results suggested an association between nuclear p16 expression and binding of proteins to NFκB as seen in mobility shift assays in cisplatin-treated cells.

Nuclear p16 Binds to NFκB—Western blot analysis of CCL23 cells showed increased nuclear expression of CDK4 and NFκB proteins when p16 activity was inhibited through the addition of p16 small-interfering RNA (p16 siRNA) (Fig. 4*A*). However, when CDK4 expression was abolished with the addition of CDK4 siRNA, the expression of NFκB was also reduced. Furthermore, immunoprecipitation studies with antibody against NFκB (p65 subunit) confirmed the binding of NFκB to both p16 and CDK4 proteins (Fig. 4*B*). Although NFκB binding to CDK4 was not affected in the presence of p16 siRNA, there was reduced binding to p16 in the presence of CDK4 siRNA. These results, therefore, suggested that p16 might interact with NFκB through a CDK4-dependent mechanism and that p16 plays a role in the negative regulation of NFκB.

Cisplatin Treatment Decreases NFκB Nuclear Expression—Immunofluorescence studies of NFκB expression in untreated CCL23 cells demonstrated cytoplasmic expression of the transcription factor at base line (*top left panel* in Fig. 4*C*), which underwent a shift to increased nuclear expression after treatment with TNF-α for 1 h. Treatment of CCL23 cells with cisplatin for 6 h resulted in decreased NFκB expression. Additionally, treatment with TNF-α for the final hour of the 6-h cisplatin treatment period still resulted in decreased nuclear translocation of NFκB. The decreased NFκB nuclear translocation after cisplatin treatment can, therefore, be correlated with the increased nuclear expression of p16 at the same time points (see Fig. 1*B*).

Nuclear p16 Expression Is Associated with Molecular Modification of NFκB—We have seen increased p16 expression in cisplatin-treated cells correlating with the appearance of a higher molecular weight NFκB band (Fig. 1*D*). To determine whether this association is present in untreated cycling HNSCC cells, nuclear expression of p16 and NFκB was evaluated at various time points of the cell cycle. We could observe an association between increased p16 expression and higher molecular weight NFκB band and reduced p16 expression and lower molecular weight NFκB (Fig. 5*A*). To confirm this association, we measured p16 and NFκB nuclear expression at different times after cisplatin treatment. We noticed increased p16 expression at 4 and 8 h that was associated with the presence of the higher molecular weight NFκB (Fig. 5*B*). At later times, reduced p16 expression was associated with the lower molecular weight NFκB bands. There was no appreciable difference in p16 expression in the cytoplasmic fraction of cisplatin-treated samples (Fig. 5*C*). Also, a single cytoplasmic 65-kDa NFκB protein was observed. These results, therefore, point to a strong association between nuclear p16 expression and molecular modification of NFκB in the nucleus of CCL23 cells. Reduced nuclear p16 expression at 12 h and later periods could be attributed to increased cell death seen 24 h after cisplatin treatment (data not shown).

To determine whether NFκB molecular modification has an effect on its transcription activity, we performed ChIP assays using the promoter sequences of IL-8, a cytokine transcribed by NFκB. Although the control input DNAs showed the 182-bp PCR product for all the cisplatin-treated samples, reduced PCR product was seen for the 4-h time period (high nuclear p16 expression; see Fig. 5*B*) in the NFκB-immunoprecipitated samples (Fig. 5*D*). These results, therefore, demonstrated removal of NFκB from its binding sites by p16 and reloading of NFκB to the DNA sites with reduction in p16 expression. The presence of 272-bp β-actin PCR product in the input and not in NFκB-immunoprecipitated samples confirmed the specificity of the ChIP assay. Additional proof for specificity was provided by the absence of IL-8 PCR product in the control IgG-immunoprecipitated samples.

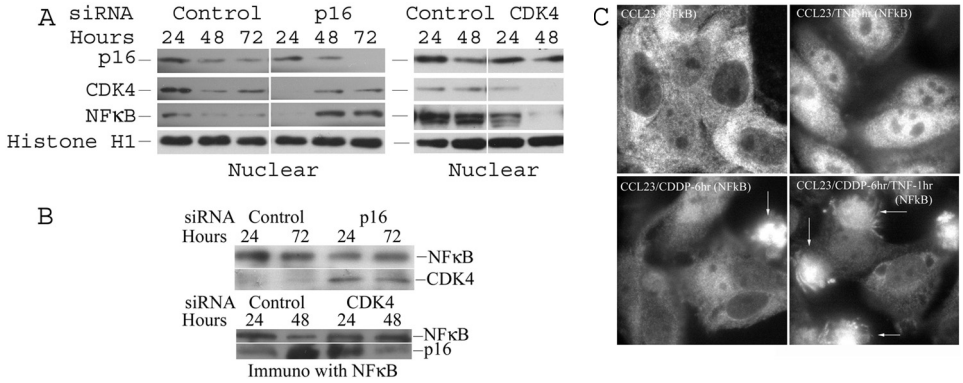

FIGURE 4. **Interaction of p16 and NFκB proteins in CCL23 cells.** *A*, nuclear expression of p16, CDK4, and NFκB is visualized in CCL23 cells. With the loss of p16 expression, levels of CDK4 and NFκB proteins are enhanced in the nucleus. However, nuclear NFκB expression seems to be reduced with the loss of CDK4 expression. *B*, NFκB antibody-immunoprecipitated proteins show binding of NFκB to CDK4 and p16 proteins. Although the binding to CDK4 is increased in the absence of p16, there is reduced binding to nuclear p16 in the absence of CDK4. These results indicate possible requirement of CDK4 for the interaction between p16 and NFκB proteins. *C*, expression of NFκB in untreated CCL23 cells is largely cytoplasmic, and treatment with TNF-α for 1 h leads to increased nuclear localization of NFκB and reduced cytoplasmic NFκB expression. However, TNF-α treatment for the final hour of cisplatin treatment of CCL23 cells does not show an increase in the level of nuclear NFκB expression, indicating possible degradation of NFκB. *Arrows* point to cells undergoing senescence/apoptosis.

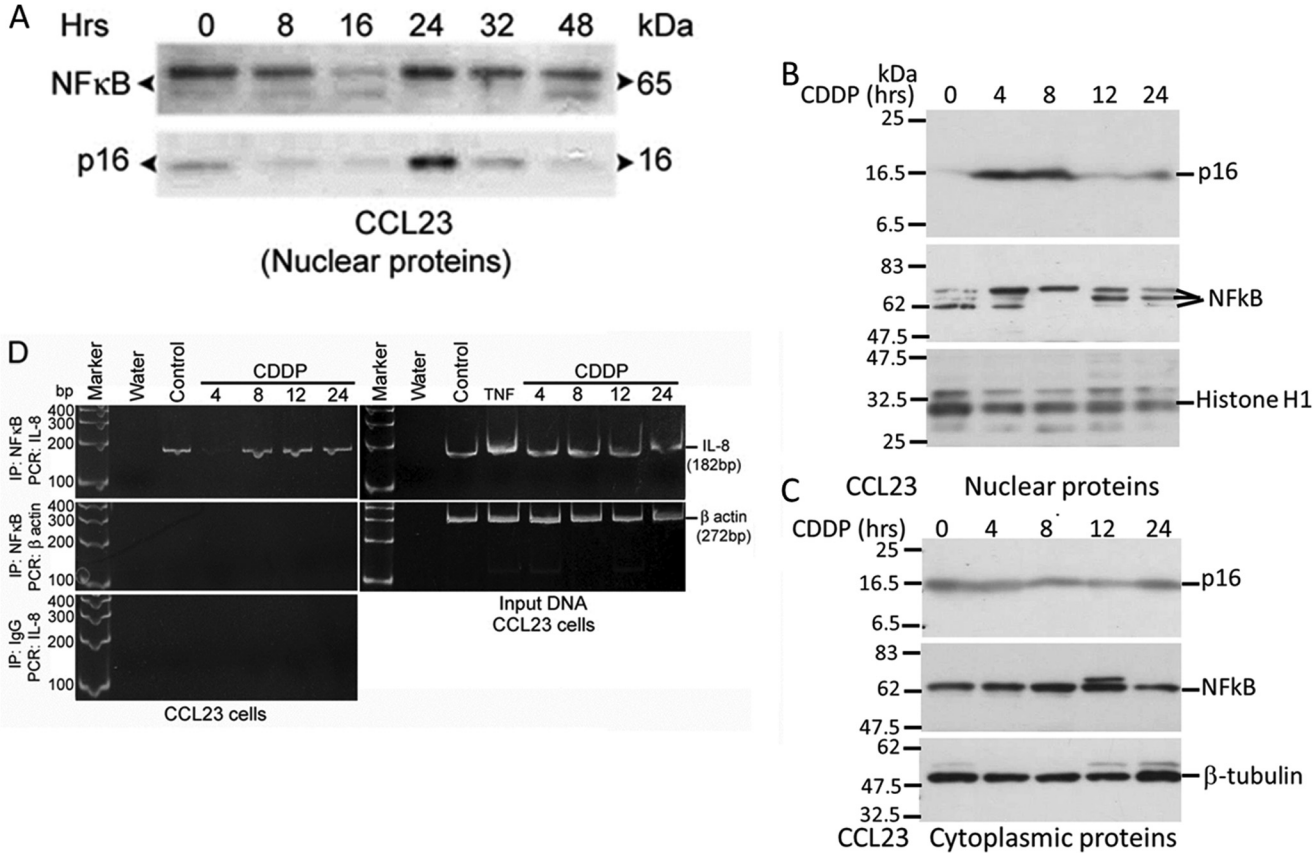

FIGURE 5. **Correlation of increased nuclear p16 expression to molecular modification of nuclear NFκB.** *A*, analysis of proteins at different times of the cell cycle shows a shift in NFκB protein mobility in relation to the level of p16-expression, higher migrating NFκB protein associated with higher expression of p16 protein. *B*, CDDP treatment of CCL23 cells results in higher p16 expression after 4 h that remains high at 8 h. NFκB shifts to the higher molecular weight form by 4 h and returns to lower molecular weight forms with reduction in p16 expression. *C*, cytoplasmic fraction of CDDP-treated samples shows a moderate difference in the expression of p16 and absence of NFκB mobility shift at different times. Histone H1 and β tubulin serve as protein loading controls for nucleus and cytoplasm, respectively. *D*, ChIP assay with primers for the IL-8 promoter indicates a reduced 182-bp PCR product at 4 h of treatment coinciding with higher level of p16 expression. The 272-bp β-actin PCR product seen in the input samples is absent in NFκB-immunoprecipitated (*IP*) samples serving as the ChIP assay control. Finally, there is no IL-8 PCR product in IgG-immunoprecipitated samples, confirming the specificity of the ChIP assay.

p16 Associates with Gigaxonin for the Ubiquitination of NFκB—To determine the proteins that are associated with the NFκB modification, we generated a doxycycline-inducible localization and affinity purification (LAP = EGFP-TEV-S-peptide)-tagged-NFκB HeLa stable cell line that expresses NFκB from a single specific loci within the genome (16). The LAP-NFκB cell line was induced with doxycycline and treated with and without cisplatin. Nuclear protein extracts were prepared, and LAP-NFκB was tandem affinity-purified (16). Western blotting and immunoprecipitation studies confirmed the

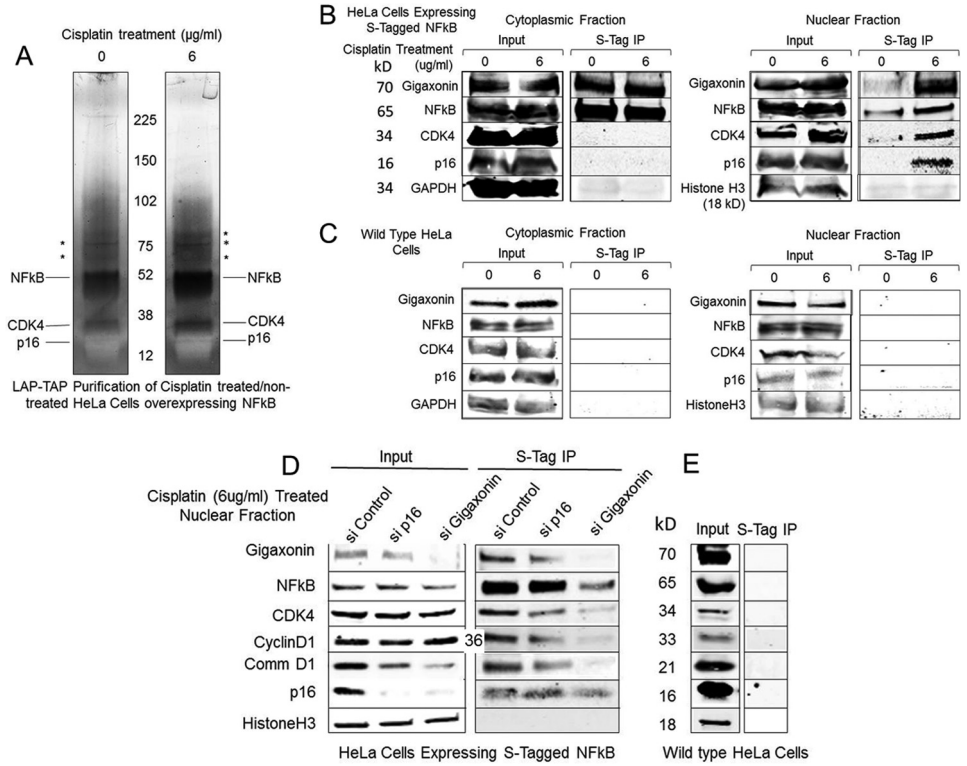

FIGURE 6. **p16 recruits gigaxonin for NFκB ubiquitination.** *A*, silver-stained 4–20% PAGE gels of the GFP-immunoprecipitated samples of the doxycycline-induced control and cisplatin-treated HeLa Flp-In T-REx EGFP-S-NFκB cells show the presence of protein bands at 50, 34, and 16 kDa, reflecting the presence of NFκB, CDK4, and p16. In addition to the 65- and 75-kDa proteins, cisplatin-treated sample shows the presence of a band at 80 kDa. A smear is also seen in the samples >50 kDa. *B*, for the identification of NFκB-interacting proteins, the cytoplasmic and nuclear lysates of doxycycline-induced control and cisplatin-treated HeLa Flp-In T-Rex EGFP-S-NFκB cells were incubated with S-protein-agarose beads. The *Input* samples representing the protein lysate before the pulldown show hybridization to all the examined proteins. Although the cytoplasmic fraction shows the presence of gigaxonin in the S-protein bead pulldown of both the control and cisplatin-treated samples, gigaxonin hybridization in the nuclear fraction is seen along with p16 hybridization only in the cisplatin-treated samples. Hybridization specificity is seen by the absence of hybridization to GAPDH in the cytoplasmic and histone H3 in the nuclear fraction of the pulldown assays. *IP*, immunoprecipitate. *C*, although NFκB, CDK4, p16, and gigaxonin are expressed in the wild type HeLa Flp-In T-Rex cells, the S-protein bead pulldown assays do not show hybridization to any of these proteins, confirming hybridization specificity. *D*, Western blot analysis of the siRNA- and cisplatin-treated nuclear samples shows reduced p16 and gigaxonin expression in the respective siRNA-treated samples. There is also a reduction in the expression of comm D1 in p16 siRNA-treated samples and that of comm D1 and p16 in gigaxonin siRNA-treated samples. The S-protein bead pulldown shows a reduction in the binding of gigaxonin and comm D1 in p16 siRNA samples, indicating the recruitment of this complex to NFκB. There is a reduction in the interaction of all examined proteins in gigaxonin siRNA samples attributable to dysregulated cytoskeletal structure in the absence of gigaxonin. *E*, absence of binding in the S-protein bead pulldown of control HeLa Flp-In T-REx cells points again to hybridization specificity.

induction of the 50-kDa protein representing the inserted 390-amino acid NFκB and its interaction with CDK4 and p16 proteins (data not shown). We then performed the LAP-TAP assay to purify the NFκB-bound proteins. Here, the LAP-TAP-purified total cell lysate immunoprecipitates of the doxycycline-induced control and cisplatin-treated cells were separated on 4–20% PAGE gels and silver-stained to identify NFκB-bound proteins. We observed the presence of 16-, 34-, and 50-kDa proteins, indicating the presence of p16, CDK4, and NFκB in the complex (Fig. 6*A*). Bands of 65 and 75 kDa were seen in control and cisplatin-treated samples, and an additional 80-kDa band was seen in cisplatin-treated samples. A smear a >50 kDa was noticed in both the control and cisplatin samples indicating the presence of ubiquitinated products.

To identify the interacting proteins, LAP-TAP-purified eluates were run to a length of 2 cm in a 4–20% SDS-PAGE gel and four 5-mm gel slices were excised, trypsinized, and analyzed by LC-MS/MS. The LAP-TAP investigation identified matches for RelA (p65 form of NFκB), ankyrin repeats reflecting the sequences present in CDK4 and p16, and chaperone Bip protein reflecting cisplatin effect (Table 2). Among the interacting proteins, we also identified gigaxonin, an ubiquitin E3 ligase adaptor involved in the ubiquitination of neuronal intermediate filaments (23). Western blot analysis confirmed the expression of gigaxonin along with NFκB, CDK4, and p16 proteins in the cytoplasmic and nuclear fractions of protein lysates of doxycycline-induced cells (Fig. 6*B*). Although the cytoplasmic gigaxonin showed interactions with NFκB in the S-peptide pulldown assays of the control and cisplatin-treated samples, nuclear interaction was seen only in cisplatin-treated samples. Although CDK4-NFκB interaction was seen in the untreated nuclear extracts, binding of p16 to the complex again occurred only in cisplatin-treated samples. Specificity of these interactions was confirmed by the absence of NFκB binding to cytoplasmic GAPDH or nuclear histone H3 (Fig. 6*B*). Additional confirmation was provided by the absence of protein bands in the immunoblots of wild type HeLa Flp-In T-Rex cell S-peptide pulldown assays (Fig. 6*C*).

To determine whether gigaxonin was recruited by p16 for NFκB ubiquitination, we performed siRNA studies. (LAP = EGFP-TEV-S-peptide)-tagged NFκB HeLa stable cell line was treated for 12 h with control, p16, or gigaxonin siRNA. Cells

TABLE 2
Proteomic MASCOT search matches for NFκB-interacting proteins
aa, amino acids. Met (O), oxidation of the methionine residue.

Gene ID	Score	Mass	Tryptic peptide matches (non-duplicates/duplicates)	Sequences searched	Gene	Modification observed
		Daltons				
gi/189504	405	60,705	39 Peptides (11/28)	11	NFκB	None
gi/15559457	402	28,216	38 Peptides (17/21)	15	RelA	None
gi/16751921	92	11,391	4 Peptides (2/2)	2	Dermcidin preproprotein	None
gi/194384240	69	59,042	5 Peptides (5/0)	5	Unnamed protein	None
gi/6470150	50	71,002	5 Peptides (5/0)	5	BiP protein, partial	None
gi553734	47	2,269	118 Peptides (1/117)	1	Putative protein	None
gi/54781221	46	13,399	2 Peptides (1/1)	1	IGg κ-variable region VK1	None
gi/113413200	40	118,740	4 Peptides (2/2)	2	POTE ankyrin domain family member J	None
gi/440575811	37	11,752	29 Peptides (1/28)	1	Alternative protein CSF2RB	None
gi/3046606	36	1,955	1 Peptide (1/0)	1	Type II interleukin 1 receptor antagonist	Acetyl (K)
gi/134133226	35	122,882	3 Peptides (2/1)	2	POTE ankyrin domain family member E	Met (O)
gi/2853301	31	100,236	1 Peptide (1/0)	1	Mucin, partial	None
gi/38051823	28	93,263	1 Peptide (1/0)	1	Plasminogen	None
gi/72534660	27	27,578	22 Peptides (1/21)	1	Serine/arginine-rich splicing factor 7 isoform 1	None
gi/107719	26	18,742	5 Peptides (1/4)	1	Sphingomyelin phosphodiesterase	None
gi/54114933	25	70,002	4 Peptides (1/3)	1	DIS3 mitotic control homologue (*s. cerevisiae*)-like 2	None
gi/11545731	25	68,678	28 Peptides (4/24)	3	Gigaxonin (597 aa)	Met (O), Ac-Lys, Tyr(P)
					Lys-412, Lys-433, and Tyr-471	
gi/13606056	25	470,227	4 Peptides (4/0)	4	DNA-dependent protein kinase catalytic subunit	None
gi/119587345	25	101,103	2 Peptides (1/1)	2	Piwi-like 4 (*Drosophila*), isoform CRA_b	Ac-Lys
gi/5734135	22	94,777	1 Peptide (1/0)	1	ATP cassette binding transporter 1	
gi/5262601	20	113,916	1 Peptide (1/0)	1	Hypothetical protein	Ac-Lys
gi/4505725	20	143,804	4 Peptides (3/1)	3	Peroxisome biogenesis factor 1	Met (O)
gi/7706681	19	139,359	2 Peptides (2/0)	2	DNA repair protein REV1 isoform 1	None
gi/410171504	19	260068	3 Peptides (2/1)	2	Hornerin	None
gi/119569105	17	11,437	23 Peptides (2/21)	1	hCG1820599	Tyr(P)

were then treated with a medium containing cisplatin (6 μg/ml) and doxycycline (0.2 μg/ml) for 4 h and then with doxycycline (0.2 μg/ml) alone medium for 32 h for a total of 48 h post-siRNA treatment. Western blot analysis of the protein lysates showed reduced expression of p16 and gigaxonin in the respective siRNA-treated samples confirming down-regulation of these two proteins with the siRNAs (Fig. 6*D*). There was also a reduced expression of comm D1 (component of the comm D1-cullin E3 ligase NFκB ubiquitination system; Ref. 11) and p16 in gigaxonin siRNA-treated samples. The S-tag pulldown assays showed a reduction in the binding of gigaxonin and comm D1 in p16 siRNA-treated samples. Interaction of NFκB with all the examined proteins was reduced in gigaxonin siRNA samples possibly due to dysregulated cytoskeletal structure in the absence of gigaxonin. Again, there was no binding of any of the proteins to S-peptide pulldown assays in the control cells confirming the specificity of protein-protein interactions (Fig. 6*E*). The absence of a clear reduction in p16 and NFκB interaction with the siRNA could be attributable to residual p16 in treated cells. This is also reflected in partial and not complete loss of gigaxonin and comm D1 binding to NFκB.

To further confirm the interaction of p16 and gigaxonin to NFκB, we performed gel shift assays. As shown earlier in Fig. 3*B*, whole cell lysates of CCL23 cells were incubated with the ^{32}P-labeled NFκB oligonucleotides, and incubation of NFκB oligonucleotides without the lysates were used as controls. Preincubation of the protein lysate with anti-p16 or anti-gigaxonin antibody resulted in a supershift of the NFκB bound oligo nucleotides (Fig. 7*A*). The supershift was, however, not observed with the anti-EGFR antibody used as an antibody isotype control. Supershift was also not observed with anti-p21 antibody, indicating the specificity of interaction between NFκB and p16 and NFκB and gigaxonin.

Because gigaxonin is an E3 ubiquitin ligase, we investigated the ubiquitination of NFκB in HeLa Flp-In T-Rex (cell line used in the LAP-TAP proteomic analysis) and CCL23 cells. Protein lysates were immunoprecipitated with NFκB and hybridized to anti-NFκB and anti-ubiquitin antibodies through a multiplex hybridization. NFκB hybridization was observed in *green* and that of ubiquitin in *red*. The analysis showed increased hybridization of the higher molecular weight bands of NFκB to the ubiquitin antibody in cisplatin treated cells in comparison to that of untreated control cells (Fig. 7*B*). Increased green and red signals pointing to enhanced NFκB ubiquitination was clearly observed in the multiplex hybridization (Fig. 7*C*). Hybridization to the ubiquitin antibody was lost in the absence of p16 and gigaxonin expression confirming the role of p16 and gigaxonin in the ubiquitination of NFκB. We, therefore, hypothesize that cisplatin treatment leads to nuclear translocation of p16, resulting in the recruitment of gigaxonin-comm D1 ubiquitin complex for the ubiquitination of NFκB (Fig. 7*D*). This would then explain reduced NFκB-DNA interaction leading to decreased transcription of cytokines and growth factors. Our results could also imply that there is a direct interaction between gigaxonin and NFκB in the nucleus that gets amplified after cisplatin treatment.

Introduction of Ectopic p16 Expression Is Not Sufficient to Increase Sensitivity of Cisplatin-resistant Cell Lines—To determine whether nuclear p16 expression was sufficient to induce cisplatin sensitivity, we performed transfection of p16 into two HNSCC cell lines: UM-SCC-14A (aggressive and cisplatin-resistant with the absence of p16 expression) and CCL23 (cisplatin-sensitive containing nuclear and cytoplasmic p16 expression) using the GALV (gibbon ape leukemia virus) retroviral vector system. Western blot analysis confirmed the expression of nuclear p16 in UM-SCC-14A-GALVp16 and enhanced

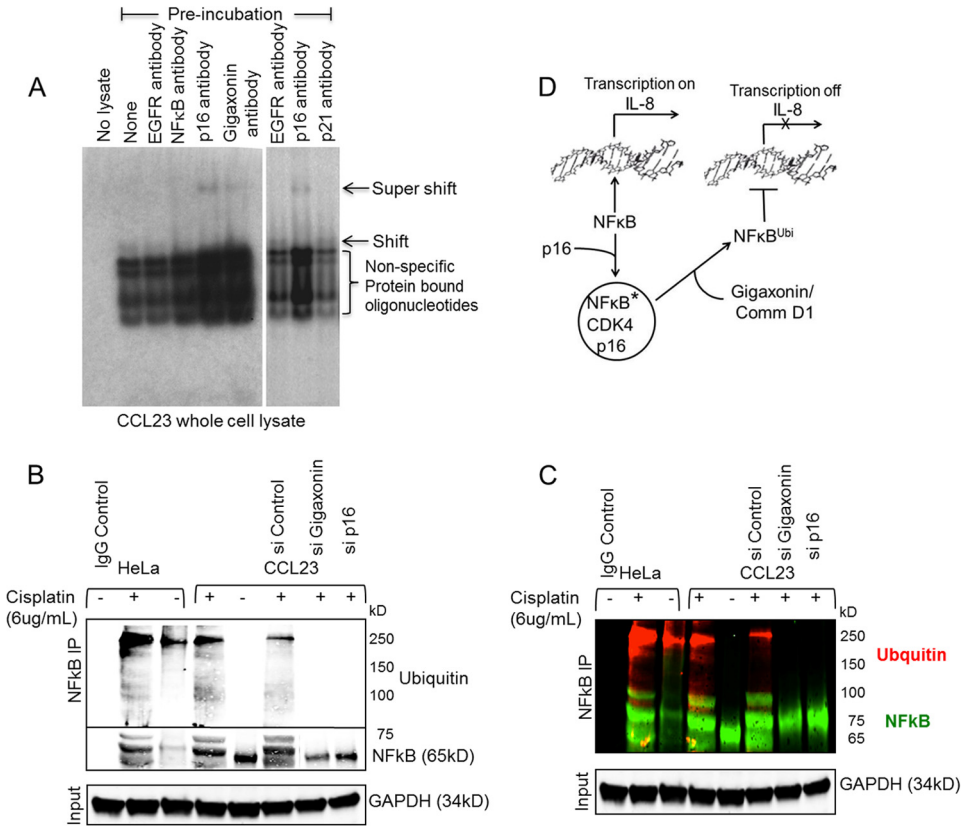

FIGURE 7. **p16 and gigaxonin mediated NFκB ubiquitination in cisplatin-sensitive cell lines.** *A*, gel shift assay shows a shift in ^{32}P-radiolabeled NFκB oligonucleotide by incubation with CCL23 whole cell protein lysates. Preincubation with anti-p16 or anti-gigaxonin antibody (both mouse monoclonal) shows a supershift pointing to the binding of p16 and gigaxonin proteins to oligonucleotide bound NFκB. Supershift was not observed by preincubation with anti-EGFR (mouse monoclonal, an isotype control) or anti-p21 (p53-induced cell cycle suppressor protein, mouse monoclonal) antibodies. We do not see shift with the NFκB antibody possibly due to a soaking effect. Incubation of the ^{32}P-radiolabeled NFκB oligonucleotide without the whole cell lysate served as the gel shift assay control. *B* and *C*, immunoprecipitation (*IP*) of whole cell protein lysates of HeLa Flp-In T-Rex EGFP-S-NFκB or CCL23 cells with NFκB followed by multiplex hybridization to NFκB and ubiquitin shows enhanced ubiquitination of NFκB in cisplatin-treated cells compared with the untreated cells. NFκB ubiquitination is lost in p16 or gigaxonin siRNA-treated samples, confirming the role of these two proteins in the ubiquitination of NFκB. *D*, molecular mechanism of control of NFκB activity with p16 expression indicating the requirement of CDK4 for the p16-NFκB interaction. Protein-protein interaction leads to molecular modification of NFκB (indicated with an *asterisk*) and ubiquitination of NFκB by gigaxonin-comm D1 complex.

expression in CCL23-GALVp16 cells (Fig. 8*A*). Immunofluorescence studies demonstrated nuclear localization of the p16 protein in the transfected cell lines (Fig. 8*B*). Growth assays demonstrated a decreased rate of proliferation in CCL23-GALVp16 cells correlating with increased p16 expression. Cell growth, however, was not affected in UM-SCC14A-GALVp16 cells in comparison to the parental cells (Fig. 8*C*). These results suggested that although nuclear p16 expression is an important factor, the effect may also require other p16-interacting proteins such as gigaxonin for the induction of cisplatin sensitivity.

Nuclear p53 Expression Is Also Associated with Cisplatin Sensitivity in HNSCC Cell Lines—We have previously shown that although the CAL27 cells lacked p16 expression and contained a mutant p53, the cells were sensitive to cisplatin (7). We showed that this was due to the nuclear localization of the p53 protein in this cell line. It is likely then that nuclear p53 is required for the cisplatin-mediated cell growth inhibition. Western blot studies indicated wild type and mutated forms of p53 expression in the cisplatin-resistant UM-SCC1, UM-SCC12, and UM-SCC14A cell lines (Fig. 9*A*). These results correlated well with exons 3 and 8 skipping in the UM-SCC1 and UM-SCC14A cells reported by Hauser *et al.* (24). Immunofluorescence analysis showed cytoplasmic localization of p53 in UM-SCC1 cells and close to background level expression in UM-SCC14A cells (Fig. 9*B*). Thus, we hypothesize that nuclear expression of p16 and/or p53 are responsible for the cisplatin-induced cell growth inhibition of head and neck cancer cells. Because we previously showed that cisplatin-induced growth arrest could involve apoptosis (7), p53-mediated growth inhibition of CAL27 might be related to apoptotic cell death.

Nuclear p16 Expression Correlates with a Favorable Clinical Prognosis in HNSCC Patients—We and others have shown inactivation of p16 by homozygous deletion and DNA methylation in 70% of HNSCC tumors (25). Little is known about the tumors with p16 expression, specifically in relationship to cytoplasmic and nuclear expression. Analysis of 103 head and neck tumors by immunohistochemistry showed p16 protein expression in 28 samples. Ten samples had cytoplasmic expression with a <1% nuclear expression. The remaining 18 samples contained nuclear expression, with 11 having >20% and 7 having expression between 4 and 20%. Expression intensity mostly correlated with percent expression, *i.e.* higher nuclear expression had higher intensity (3+ to 4+), and lower expression had <2+ intensity. The relationship to survival was, therefore, calculated with respect to the percentage of expression. The analyses

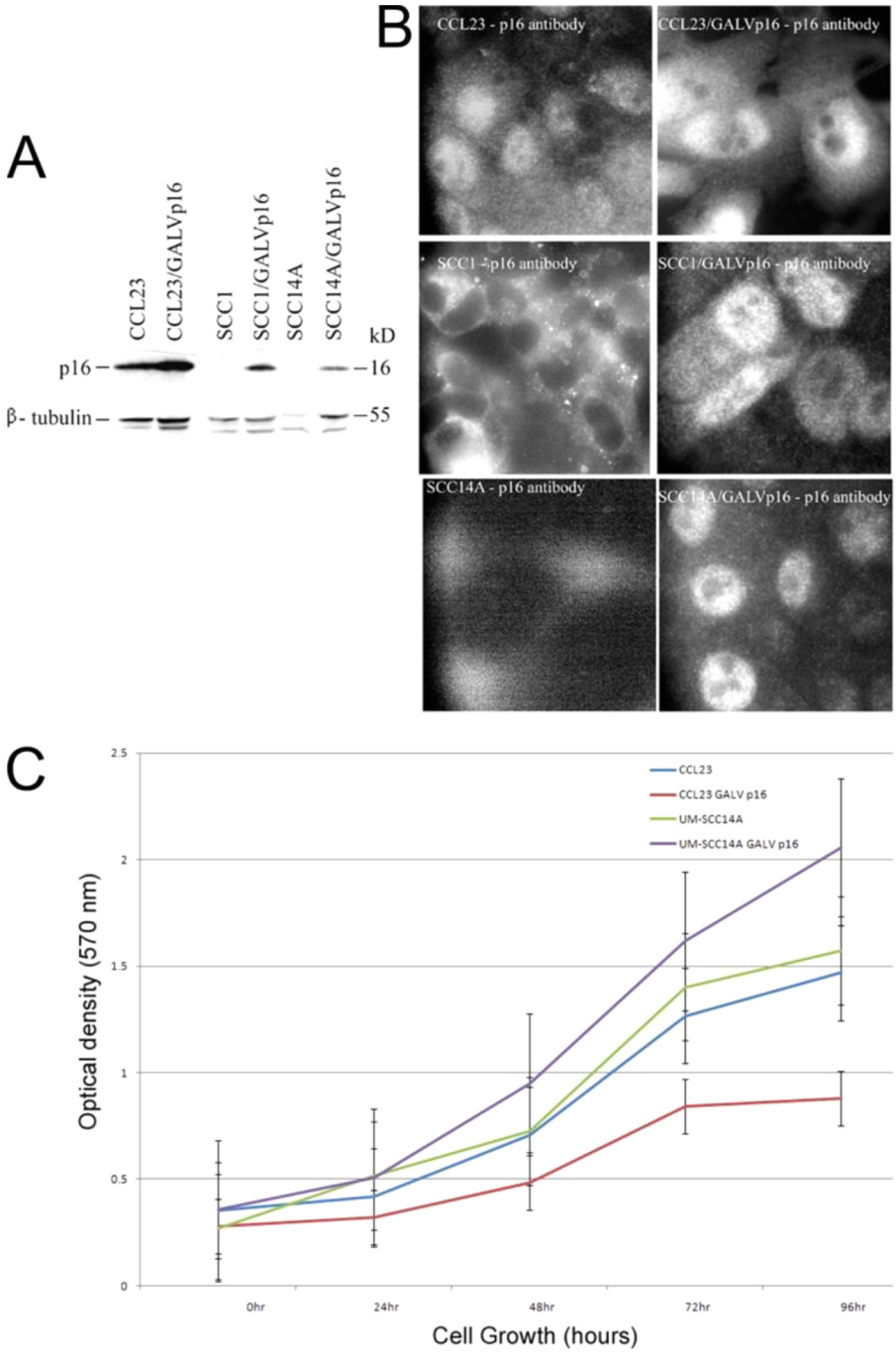

FIGURE 8. **Absence of growth inhibition with ectopic p16 expression in UM-SCC14A cells.** *A*, Western blot analysis demonstrates increased p16 expression in GALVp16 transfected cells. *B*, immunofluorescence studies confirm localization of p16 to the nucleus of the cell lines. *C*, growth assays for the cell lines demonstrate reduced cell growth in CCL23-GALVp16 cells relative to the CCL23 control (p value <0.05). However, the growth rate of UM-SCC14A-GALVp16 is not affected with respect to the control UM-SCC14A cells as a result of increased p16 expression (p value < 0.38).

showed significantly longer overall survival for patients with higher levels of nuclear p16 expression ($p < 0.0000542$), an effect likely related to increased cisplatin sensitivity (Fig. 10*A*). Western blot analysis of an independent set of primary tumors showed an inverse relationship between the expression of p16 and that of CDK4 and NFκB (Fig. 10*B*). Although tumors with p16 expression showed reduced expression of CDK4 and NFκB (as seen in tumor samples 18 and 40), loss of p16 was accompanied by overexpression of CDK4 and NFκB (demonstrated in tumor samples 26, 54, 91, 222, 277, and 295).

Association of HPV with Nuclear p16 Expression in HNSCC Tumors—In recent years, HPVs have also been implicated in head and neck cancers (26, 27). Tumors with HPV positivity, known as basaloid (laryngeal and pharyngeal) tumors, are shown to have a better prognosis, *i.e.* increased sensitivity to chemoradiation therapies (27). To determine the relationship between p16 expression and the presence of HPVs, five each of basaloid, primary, and recurrent head and neck tumors were analyzed for the expression of p16, IL-8, macrophage marker CD68, and cancer stem cell markers (related to tumor aggres-

siveness) BMI-1, CD44, and ALDH-1. Four of the basaloid tumors contained enhanced p16 nuclear expression accompanied by lower expression of CD68, IL-8, and cancer stem cell markers (Fig. 11*A* and Table 3). Primary and recurrent tumors were devoid of p16 expression but showed higher expression of all the examined markers (Fig. 11*B*). Recurrent tumors also showed expression of CD68 and IL-8 in the tumor clusters indicating a tumor immune response (Fig. 12). These results suggested a direct correlation between HPV and p16 expression and an inverse relationship between HPV and the expression of IL-8 and CD68, indicating an inverse relationship between HPV and tumor-associated immune response.

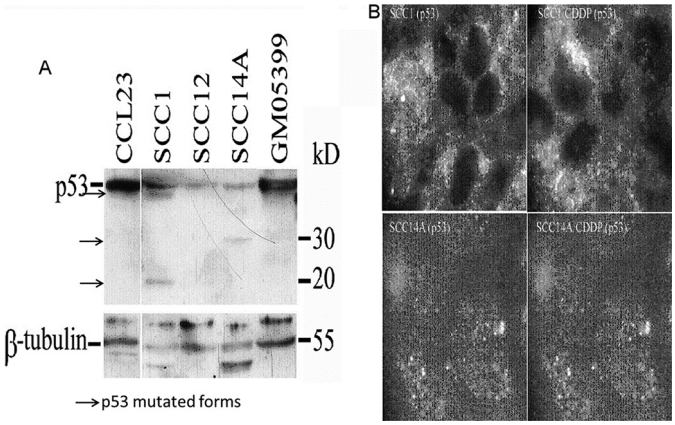

FIGURE 9. **Expression of mutant p53 proteins in cisplatin-resistant cell lines.** *A*, Western blot analysis shows the presence of wild type p53 protein in CCL23 cells. However, low molecular weight mutant p53 proteins are seen in UM-SCC1 and UM-SCC14A cell lines. These cell lines also contain low level expression of a 53-kDa protein indicating the presence of an unstable p53 protein. *B*, immunofluorescence analysis shows cytoplasmic p53 expression in UM-SCC1 and UM-SCC14A cells that is not translocated to the nucleus upon the addition of CDDP.

DISCUSSION

Platinum-based agents are the standard of care in chemotherapeutic regimens for HNSCC. However, cisplatin and its related drugs alone are not effective for the treatment of head and neck cancers. The efficacy of cisplatin in HNSCC is significantly increased in combination with other chemotherapeutic agents and/or radiation therapy (28–30). A key event mediating the cellular toxicity of cisplatin is the formation of DNA cross-links. After adduct formation via replacement of the chloride ligands of the drug with DNA bases, further replication and transcription is halted, and cells are stimulated to undergo apoptosis (31). In addition to triggering apoptosis, several studies have shown that cisplatin induces cellular senescence, as evidenced by expression of the senescence-associated marker β-galactosidase (32, 33). However, the mechanism of cisplatin-induced cellular senescence is not known. Investigations into the mode of action of cisplatin have, therefore, focused on key regulators of the cell cycle and apoptosis such as p16 and p53 proteins (34–36).

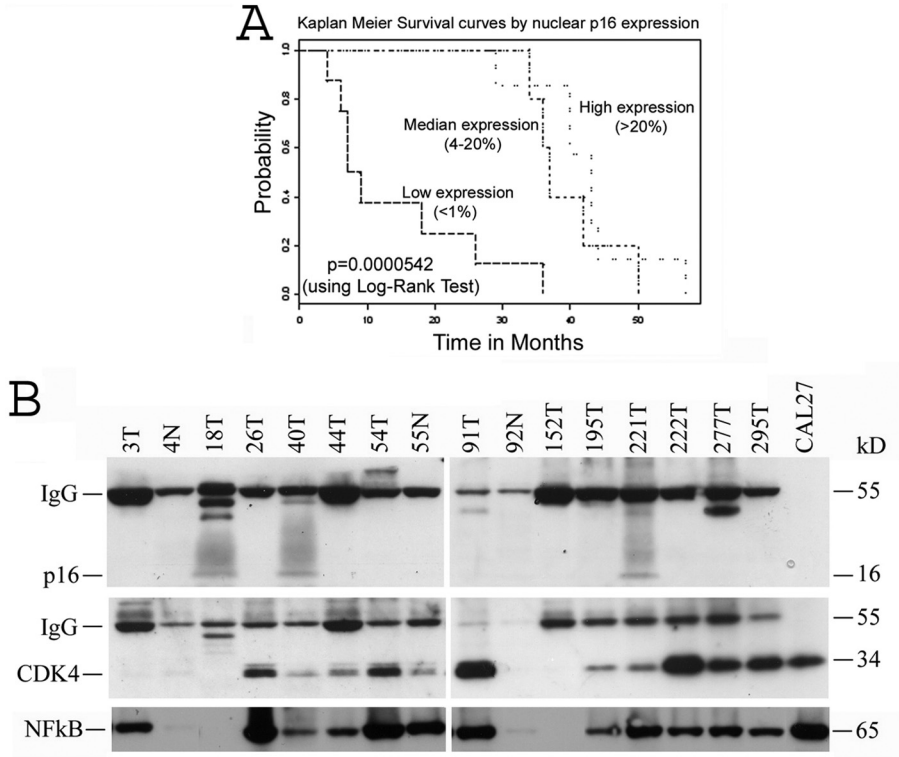

FIGURE 10. **Nuclear p16 expression correlates with a favorable prognosis in HNSCC patients.** *A*, Kaplan-Meier curves showing the association of nuclear p16 expression with patient survival in 103 tumor samples demonstrating longer survival for patients with higher nuclear expression (p value < 0.0000542). *B*, Western blot analysis of 13 primary tumor samples and three normal tissues shows p16 expression in three tumors (*18T*, *40T*, and *221T*). Two of these tumors (18T and 40T) have reduced expression of CDK4 and NFκB. Loss of p16 expression in seven tumors is accompanied by increased expression of CDK4 and NFκB. CAL27 cells without p16 expression also contain higher levels of expression of CDK4 and NFκB. Thus, there is an inverse relationship between the expression of p16 and that of CDK4 and NFκB in head and neck tumors. Normal tissues contain low level expression of all three proteins. Hybridization to IgG is used as an internal control for protein loading.

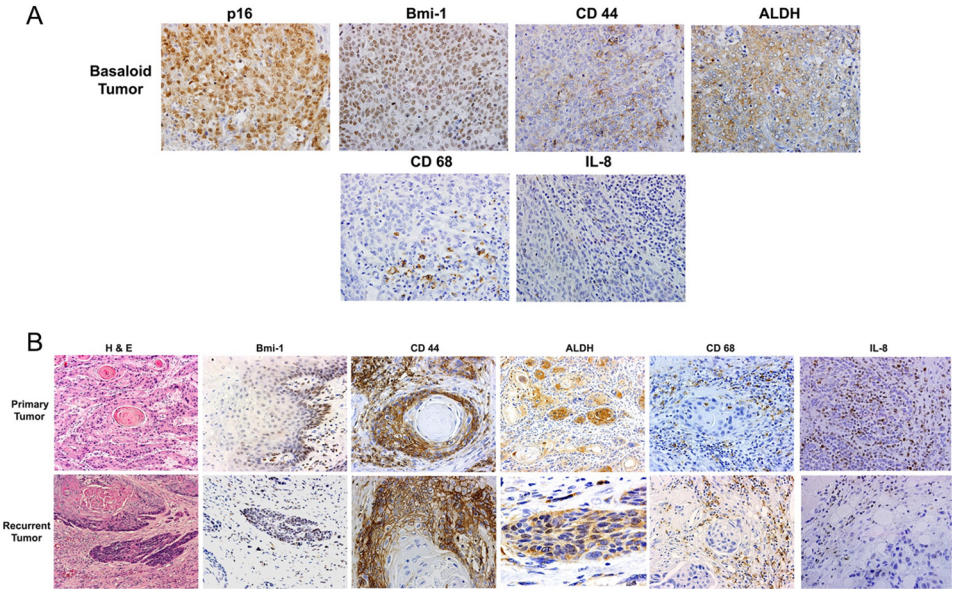

FIGURE 11. **Inverse relationship between p16 and IL-8.** *A*, HPV-positive basaloid tumors show p16 expression and low level expression of IL-8, CD68 (macrophage marker) and cancer stem cell markers. *B*, HPV negative primary and recurrent tumors do not express p16. However, they show higher expression of CD68 and cancer stem markers. In the recurrent tumors expression CD68 and IL-8 is seen in tumor cell clusters indicating higher immune response at the tumor sites.

Studies correlating the level of p16 expression and response to platinum-based chemotherapy in various cancers have pointed to an association between p16 deletion and cisplatin resistance (37). A retrospective investigation of ovarian cancer patients revealed a significantly higher frequency of p16 deletion in tumors that did not respond to cisplatin chemotherapy (37). It was demonstrated in non-small cell lung cancer that p16 is involved in mediating G_1 cell cycle arrest and apoptosis in response to treatment with irradiation, DNA topoisomerase inhibitors, and cisplatin (38, 39). We have previously shown that cisplatin treatment in HNSCC cells was associated with increased expression of p16 and p53, suggesting that cisplatin-induced cell cycle arrest operates through the p16/p53-dependent pathways (7).

Multiple studies have shown that functional p53 is necessary for chemotherapy-induced apoptosis; several investigations in HNSCC have found that cell lines with p53 mutations demonstrate increased sensitivity to cisplatin (40–42). These findings may not actually be in conflict, as p53 mutations that do not affect nuclear localization of the protein were noted to increase sensitivity to cisplatin, whereas mutations associated with loss of nuclear p53 predicted a poor response to chemotherapy (40–42). Overall, the data in multiple cancers including HNSCC support the role of functional p53 expression in predicting a positive response to platinum-based chemotherapy.

The regulation of cyclin D1 expression is controlled through NFκB, an inducible transcription factor that also regulates a host of gene products involved in inflammation and cellular proliferation including cyclooxygenase-2, IκBα, TNF-α, cyclin E, ICAM-1, c-myc, Bcl-2, MMP-9, inducible nitric-oxide synthase (iNOS), and interleukins including IL-6 and IL-8 (8–10). NFκB is a nuclear factor that has been widely studied for its role in cancer development and growth. Investigations have shown an increased inflammatory response in association with the growth and metastasis of both hematologic and solid malignancies (43–45). It has also been shown that the up-regulated expression of tumor-promoting cytokines IL-6, IL-8, and TNF-α in various cancers is the result of increased activation of NFκB (46). In addition, it has also been shown that NFκB expression is associated with the development of cancer stem cells related to chemoradiation resistance in several malignancies including head and neck, colon, and prostate cancers (47). Therefore, understanding the control of NFκB activation pathways represents an important target in the area of cancer prevention and therapy.

Studies in animal models of human cancer have supported the role of the inflammatory cascade in cancer progression. Investigations in melanoma, lung, and prostate cancers have shown that modulation of NFκB activity via inhibition of IκKα/IκKβ has the potential to suppress tumor growth and metastasis (48, 49). In head and neck cancer, we and others have demonstrated that inhibition of IκKβ leads to suppression of HNSCC growth (50). However, the precise molecular mechanism of this NFκB-mediated growth-suppressive effect of cisplatin in human cancers is not yet understood.

In the present investigation we provide a mechanism for cellular apoptosis and senescence mediated by cisplatin treatment of head and neck cancers. This involves targeting of NFκB for ubiquitination by p16 through the recruitment of gigaxonin (Fig. 7*D*). Gigaxonin was identified because of mutations of the GAN gene (coding for gigaxonin) in giant axonal neuropathies, an early onset neuronal disorder (23, 51). Gigaxonin belongs to the BTB-KELCH family of adaptor proteins where the KELCH domain interacts with the protein targeted for degradation and BTB domain interacts with the E3 ubiquitin ligase complex. In the absence of a functional gigaxonin, aggregates of vimentin intermediate filaments in fibroblasts and aggregates of peripherin and neurofilament intermediate filaments in neurons have been documented (23). These studies have implicated gigaxonin in the ubiquitination of intermediate filaments for the for-

TABLE 3
Expression status of stem cell markers in HNSCC tumor samples

Sample	Tumor	ALDH	BMI-1	CD 44	CD 68	IL-8	p16
1	Primary	70%, Cytoplasmic	80%, diffuse, nuclear staining, cellular stains and keratinization does not stain	90% Membrane, diffuse	Macrophages mostly at periphery of tumor nests (100%)	Not done	Negative
2	Primary	100%, Diffuse, basal layer	60–70%, basal epithelium, more at periphery and poor diff areas	More at periphery, less at keratinization areas	Macrophages mostly at periphery of tumor nests (100%)	Scattered IL-8 + inflammatory cells mostly at periphery of tumor nests (100%)	Negative
3	Primary	Scattered, focal positivity	Diffuse, strong	90%, Diffuse	Macrophages mostly at periphery of tumor nests (100%)	Scattered IL-8 + inflammatory cells mostly at periphery of tumor nests (100%)	Negative
4	Primary	5%, Scattered, individual cells	Diffuse, strong	90%, Diffuse	Macrophages mostly at periphery of tumor nests (100%)	Not done	
5	Primary	5%, Scattered	Diffuse, strong	90%, Diffuse	Macrophages mostly at periphery of tumor nests (100%)	Not done	
6	Recurrent	Faint, weak, more at periphery	50%, Weaker	90%, Diffuse, more at periphery, less at center	Macrophages present within necrotic centers (60%) and at periphery (40%) of tumor nests	Scattered IL-8 + inflammatory cells within center (30%) and at periphery (70%) of tumor nests	Negative
7	Recurrent	Diffuse, more basal layer	Diffuse, basal layer	Diffuse, peripheral staining	Macrophages present within necrotic centers (70%) and at periphery (30%) of tumor nests	Scattered IL-8 + inflammatory cells within center (50%) and at periphery (50%) of tumor nests	Negative
8	Recurrent	Strong at periphery and basal layer, cytoplasmic in tumor	Weaker, positive at periphery	Diffuse, peripheral staining	Macrophages present within necrotic centers (20%) and at periphery (80%) of tumor nests	Scattered IL-8 + inflammatory cells within center (30%) and at periphery (70%) of tumor nests	Positive
9	Recurrent	Faint, diffuse staining	Diffuse, strong	90%, Diffuse	Macrophages mostly at periphery of tumor nests (100%)	Not done	Negative
10	Recurrent	Mild staining, smaller tumor	Weak, faint, stain basal layer	Strongly positive within tumor	Macrophages mostly at periphery of tumor nests (100%)	Scattered IL-8 + inflammatory cells mostly at periphery of tumor nests (100%)	Negative
11	Basaloid	>75%, Cytoplasmic, weak-to-moderate	Diffuse, nuclear, weak	25–49%, Membranous, weak	Macrophages mostly at periphery of tumor nests (100%)	Scattered IL-8 + inflammatory cells mostly at periphery of tumor nests (100%)	Positive
12	Basaloid	<25%, Cytoplasmic, weak	Diffuse, nuclear, strong	25–49%, Membranous, moderate-to-strong	Macrophages present within necrotic centers (30%) and at periphery of tumor nests (70%)	Few scattered IL-8 + inflammatory cells mostly at periphery of tumor nests (100%)	Positivee
13	Basaloid	50–74%, Cytoplasmic, moderate-to-strong	<25%, nuclear, weak	50–74%, Membranous, strong	Macrophages present within necrotic centers (25%) and at periphery (75%) of tumor nests	Few scattered IL-8 + inflammatory cells within central necrotic areas; no appreciable IL-8 + cells at periphery	Positive
14	Basaloid	50–75%, Cytoplasmic, weak-to-moderate	Diffuse, nuclear, moderate-to-strong	Not done	Macrophages present within necrotic centers (10%) and at periphery (90%) of tumor nests	Scattered IL-8 + inflammatory cells mostly at periphery of tumor nests (100%)	Positive
15	Basaloid	<25%, Cytoplasmic, weak	Diffuse, nuclear, weak	50–74%, Membranous, strong	Macrophages mostly at periphery of tumor nests (100%)	Few scattered IL-8 + inflammatory cells mostly at periphery of tumor nests (100%)	Negative

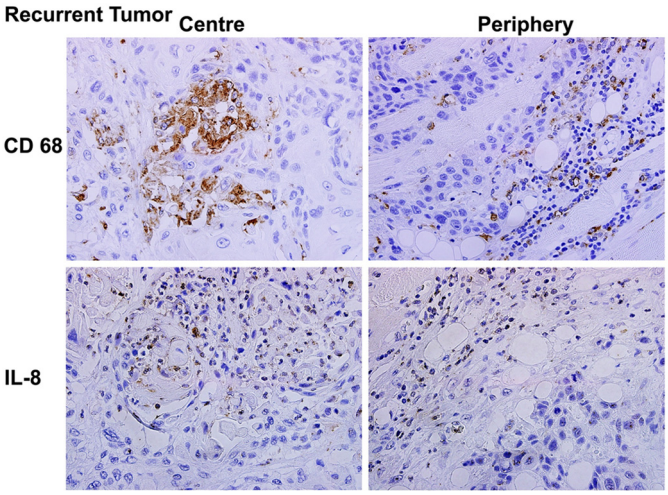

FIGURE 12. **Expression of CD68 and IL-8 in tumor clusters of recurrent tumors.** The presence of CD68 and IL-8 in tumor clusters as well as in the periphery of tumor cells is shown to indicate the presence of macrophages and the expression of cytokines in between tumor cells of recurrent tumors.

mation of neuronal cytoskeletal structures. For the first time we demonstrate that gigaxonin is expressed in cancer cell lines and is recruited for NFκB degradation by p16.

It is well known that p16 positivity is associated with the presence of oncogenic HPV and better clinical outcome for patients with head and neck cancer (52, 53). Thus, p16 expression is routinely used as a surrogate marker of HPV and chemoradiation treatment. A number of investigations are, therefore, focused on the identification of prognostic markers and the molecular mechanism of chemoradiation response in HPV positive and negative tumors. In one of the studies of oropharyngeal cancer related to betel nut chewing, it has been shown that besides p16 and HPV positivity, lower expression of p53 and the absence of EGFR expression are also associated with good clinical outcome (54). Inhibitors of mTOR (everolimus) and tyrosine kinase (sorafenib and sunitinib) signaling pathways have shown a significant growth inhibitory effect on a HPV positive tumor cell line (55). Although the drugs were less effective in HPV negative tumor cell lines, a reduction in the expression of HIF-1α was seen indicating the presence of hypoxic cells. Patient studies have shown a better clinical outcome for radiotherapy combined with nimorazole, an inhibitor of hypoxia in HPV-negative tumors (55, 56). Compared with radiotherapy alone, HPV-positive tumors did not show improved outcome when radiotherapy was combined with nimorazole, indicating the absence of hypoxic cells in HPV-positive tumors.

We have seen an association between the down-regulation of NFκB and reduced expression of inflammation-associated proteins in p16 positive primary tumors. This could be related to poor immune response and HPV infection of the tumor cells. In the absence of p16 expression, active cellular immune response in aggressive tumors could lead to the recruitment of macrophages to the tumor sites, which in turn could inhibit HPV infection. The role of tumor-associated macrophages in tumor aggressiveness and metastasis is known (57). M2 phenotype of tumor-associated macrophage regulates NFκB activity through autophagy leading to growth suppression (58). However, the relationship between NFκB activation and development of tumor promoting M2 phenotype is not known. We believe that the gigaxonin effect on intermediate filaments and microtubule assembly could activate autophagy. In the absence of gigaxonin, microtubule reorganization could result in the suppression of autophagy and the development of tumor-promoting M2 phenotype. We, therefore, hypothesize that nuclear expression of p16 and gigaxonin could serve as useful markers of chemosensitivity in head and neck cancers.

REFERENCES

1. Ferlay, J., Soerjomataram, I., Dikshit, R., Eser, S., Mathers, C., Rebelo, M., Parkin, D.M., Forman, D., and Bray, F. (2014) Cancer incidence and mortality worldwide: sources, methods, and major patterns in GLOBOCAN 2012. *Int. J. Cancer* 10.1002/ijc.29210
2. Altekruse, S. F., Kosary, C. L., and Krapcho, M. (eds) *SEER Cancer Statistics Review,* 1975–2007, National Cancer Institute, Bethesda, MD
3. Lucs, A. V., Saltman, B., Chung, C. H., Steinberg, B. M., and Schwartz, D. L. (2013) Opportunities and challenges facing biomarker development for personalized head and neck cancer treatment. *Head Neck* **35,** 294–306
4. Braakhuis, B. J., Brakenhoff, R. H., and Leemans, C. R. (2012) Treatment choice for locally advanced head and neck cancers on the basis of risk factors: biological risk factors. *Ann. Oncol.* **23,** 173–177
5. Xu, J., He, X., Cheng, K., Guo, W., Bian, X., Jiang, X., Zhang, L., and Huang, S. (2014) Concurrent chemoradiotherapy with nedaplatin plus paclitaxel or fluorouracil for locoregionally advanced nasopharyngeal carcinoma: survival and toxicity. *Head Neck* **36,** 1474–1480
6. Martins, R. G., Parvathaneni, U., Bauman, J. E., Sharma, A. K., Raez, L. E., Papagikos, M. A., Yunus, F., Kurland, B. F., Eaton, K. D., Liao, J. J., Mendez, E., Futran, N., Wang, D. X., Chai, X., Wallace, S. G., Austin, M., Schmidt, R., and Hayes, D. N. (2013) Cisplatin and radiotherapy with or without erlotinib in locally advanced squamous cell carcinoma of the head and neck: a randomized phase II trial. *J. Clin. Oncol.* **31,** 1415–1421
7. Yip, H. T., Chopra, R., Chakrabarti, R., Veena, M. S., Ramamurthy, B., Srivatsan, E. S., and Wang, M. B. (2006) Cisplatin-induced growth arrest of head and neck cancer correlates with increased expression of p16 and p53. *Arch. Otolaryngol. Head Neck Surg.* **132,** 317–326
8. Barnes, P. J., and Karin, M. (1997) Nuclear factor-κB, a pivotal transcription factor in chronic inflammatory diseases. *N. Engl. J. Med.* **336,** 1066–1071
9. Garg, A., and Aggarwal, B. B. (2002) Nuclear transcription factor-κB as a target for cancer drug development. *Leukemia* **16,** 1053–1068
10. Ghosh, S., and Karin, M. (2002) 0 Missing pieces of the NF-κB puzzle. *Cell* **109,** S81–S96
11. van de Sluis, B., Mao, X., Zhai, Y., Groot, A. J., Vermeulen, J. F., van der Wall, E., van Diest, P. J., Hofker, M. H., Wijmenga, C., Klomp, L. W., Cho, K. R., Fearon, E. R., Vooijs, M., and Burstein, E. (2010) COMMD1 disrupts HIF-1α/β dimerization and inhibits human tumor cell invasion. *J. Clin. Invest.* **120,** 2119–2130
12. Anto, R. J., Mukhopadhyay, A., Shishodia, S., Gairola, C. G., and Aggarwal, B. B. (2002) Cigarette smoke condensate activates nuclear transcription factor-κB through phosphorylation and degradation of IκB(α): correlation with induction of cyclooxygenase-2. *Carcinogenesis* **23,** 1511–1518
13. Kordes, U., Krappmann, D., Heissmeyer, V., Ludwig, W. D., and Scheidereit, C. (2000) Transcription-factor NF-κB is constitutively activated in acute lymphoblastic leukemia cells. *Leukemia* **14,** 399–402
14. Wang, W., Abbruzzese, J. L., Evans, D. B., Larry, L., Cleary, K. R., and Chiao, P. J. (1999) The nuclear factor-κB RelA transcription factor is constitutively activated in human pancreatic adenocarcinoma cells. *Clin. Cancer Res.* **5,** 119–127
15. Ondrey, F. G., Dong, G., Sunwoo, J., Chen, Z., Wolf, J. S., Crowl-Bancroft, C. V., Mukaida, N., and Van Waes, C. (1999) Constitutive activation of transcription factors NF-κB, AP-1, and NF-IL6 in human head and neck squamous cell carcinoma cell lines that express pro-inflammatory and pro-angiogenic cytokines. *Mol. Carcinog.* **26,** 119–129
16. Torres, J. Z., Miller, J. J., and Jackson, P. K. (2009) High-throughput gen-

eration of tagged stable cell lines for proteomic analysis. *Proteomics* **9,** 2888–2891
17. Duarte, V. M., Han, E., Veena, M. S., Salvado, A., Suh, J. D., Liang, L. J., Faull, K. F., Srivatsan, E. S., and Wang, M. B. (2010) Curcumin enhances the effect of cisplatin in suppression of head and neck squamous cell carcinoma via inhibition of IKKβ protein of the nuclear factor kB pathway. *Mol. Cancer. Ther.* **9,** 2665–2675
18. LoTempio, M. M., Veena, M. S., Steele, H. L., Ramamurthy, B., Ramalingam, T. S., Cohen, A. N., Chakrabarti, R., Srivatsan, E. S., and Wang, M. B. (2005) Curcumin suppresses growth of head and neck squamous cell carcinoma. *Clin. Cancer Res.* **11,** 6994–7002
19. Basak, S. K., Veena, M. S., Oh, S., Lai, C., Vangala, S., Elashoff, D., Fishbein, M. C., Sharma, S., Rao, N. P., Rao, D., Phan, R., Srivatsan, E. S., and Batra, R. K. (2013) The $CD44^{high}$ tumorigenic subsets in lung cancer biospecimens are enriched for low miR-34a expression. *PLoS ONE* **8,** e73195
20. Kato, J., Matsushime, H., Hiebert, S. W., Ewen, M. E., and Sherr, C. J. (1993) Direct binding of cyclin D to the retinoblastoma gene product (pRb) and pRb phosphorylation by the cyclin D-dependent kinase CDK4. *Genes Dev.* **7,** 331–342
21. Delston, R. B., and Harbour, J. W. (2006) Rb at the interface between cell cycle and apoptotic decisions. *Curr. Mol. Med.* **6,** 713–718
22. Becker, T. M., Rizos, H., de la Pena, A., Leclercq, I. A., Woodruff, S., Kefford, R. F., and Mann, G. J. (2005) Impaired inhibition of NFκB activity by melanoma-associated p16INK4a mutations. *Biochem. Biophys. Res. Commun.* **332,** 873–879
23. Mahammad, S., Murthy, S. N., Didonna, A., Grin, B., Israeli, E., Perrot, R., Bomont, P., Julien, J. P., Kuczmarski, E., Opal, P., and Goldman, R. D. (2013) Giant axonal neuropathy-associated gigaxonin mutations impair intermediate filament protein degradation. *J. Clin. Invest.* **123,** 1964–1975
24. Hauser, U., Balz, V., Carey, T. E., Grénman, R., Van Lierop, A., Scheckenbach, K., and Bier, H. (2002) Reliable detection of p53 aberrations in squamous cell carcinomas of the head and neck requires transcript analysis of the entire coding region. *Head Neck* **24,** 868–873
25. Namazie, A., Alavi, S., Olopade, O. I., Pauletti, G., Aghamohammadi, N., Aghamohammadi, M., Gornbein, J. A., Calcaterra, T. C., Slamon, D. J., Wang, M. B., and Srivatsan, E. S. (2002) Cyclin D1 amplification and p16 (MTS1/CDK4I) deletion correlate with poor prognosis in head and neck tumors. *Laryngoscope* **112,** 472–481
26. Kreimer, A. R., Clifford, G. M., Boyle, P., and Franceschi, S. (2005) Human papillomavirus types in head and neck squamous cell carcinomas worldwide: a systematic review. *Cancer Epidemiol. Biomarkers. Prev.* **14,** 467–475
27. Mooren, J. J., Gültekin, S. E., Straetmans, J. M., Haesevoets, A., Peutz-Kootstra, C. J., Huebbers, C. U., Dienes, H. P., Wieland, U., Ramaekers, F. C., Kremer, B., Speel, E. J., and Klussmann, J. P. (2014) P16INK4A immunostaining is a strong indicator for high-risk-HPV-associated oropharyngeal carcinomas and dysplasias but is unreliable to predict low risk HPV infection in head and neck papillomas and laryngeal dysplasias. *Int. J. Cancer* **134,** 2108–2117
28. Benasso, M. (2013) Induction chemotherapy for squamous cell head and neck cancer: a neverending story? *Oral Oncol.* **49,** 747–752
29. Gupta, S., Khan, H., Barik, S., and Negi, M. P. (2013) Clinical benefits of concurrent capecitabine and cisplatin *versus* concurrent cisplatin and 5-flurouracil in locally advanced squamous cell head and neck cancer. *Drug Discov. Ther.* **7,** 36–42
30. Lefebvre, J. L., Pointreau, Y., Rolland, F., Alfonsi, M., Baudoux, A., Sire, C., de Raucourt, D., Malard, O., Degardin, M., Tuchais, C., Blot, E., Rives, M., Reyt, E., Tourani, J. M., Geoffrois, L., Peyrade, F., Guichard, F., Chevalier, D., Babin, E., Lang, P., Janot, F., Calais, G., Garaud, P., and Bardet, E. (2013) Induction chemotherapy followed by either chemoradiotherapy or bioradiotherapy for larynx preservation: the TREMPLIN randomized phase II study. *J. Clin. Oncol.* **31,** 853–859
31. Trimmer, E. E., and Essigmann, J. M. (1999) Cisplatin. *Essays Biochem.* **34,** 191–211
32. Gewirtz, D. A., Holt, S. E., and Elmore, L. W. (2008) Accelerated senescence: an emerging role in tumor cell response to chemotherapy and radiation. *Biochem. Pharmacol.* **76,** 947–957
33. Havelka, A. M., Berndtsson, M., Olofsson, M. H., Shoshan, M. C., and Linder, S. (2007) Mechanisms of action of DNA-damaging anticancer drugs in treatment of carcinomas: is acute apoptosis an "off-target" effect? *Mini Rev. Med. Chem.* **7,** 1035–1039
34. Fang, K., Chiu, C. C., Li, C. H., Chang, Y. T., and Hwang, H. T. (2007) Cisplatin-induced senescence and growth inhibition in human non-small cell lung cancer cells with ectopic transfer of p16INK4a. *Oncol. Res.* **16,** 479–488
35. Sorenson, C. M., Barry, M. A., and Eastman, A. (1990) Analysis of events associated with cell cycle arrest at G_2 phase and cell death induced by cisplatin. *J. Natl. Cancer Inst.* **82,** 749–755
36. Gallagher, W. M., Cairney, M., Schott, B., Roninson, I. B., and Brown, R. (1997) Identification of p53 genetic suppressor elements which confer resistance to cisplatin. *Oncogene* **14,** 185–193
37. Kudoh, K., Ichikawa, Y., Yoshida, S., Hirai, M., Kikuchi, Y., Nagata, I., Miwa, M., and Uchida, K. (2002) Inactivation of p16/CDKN2 and p15/MTS2 is associated with prognosis and response to chemotherapy in ovarian cancer. *Int. J. Cancer* **99,** 579–582
38. Al-Mohanna, M. A., Manogaran, P. S., Al-Mukhalafi, Z., A Al-Hussein, K., and Aboussekhra, A. (2004) The tumor suppressor p16(INK4a) gene is a regulator of apoptosis induced by ultraviolet light and cisplatin. *Oncogene* **23,** 201–212
39. Shapiro, G. I., Edwards, C. D., Ewen, M. E., and Rollins, B. J. (1998) p16INK4A participates in a G_1 arrest checkpint in response to DNA damage. *Mol. Cell. Biol.* **18,** 378–387
40. Fouret, P., Temam, S., Charlotte, F., and Lacau-St-Guily, J. (2002) Tumour stage, node stage, p53 gene status, and bcl-2 protein expression as predictors of tumour response to platin-fluorouracil chemotherapy in patients with squamous-cell carcinoma of the head and neck. *Br. J. Cancer* **87,** 1390–1395
41. Bradford, C. R., Zhu, S., Ogawa, H., Ogawa, T., Ubell, M., Narayan, A., Johnson, G., Wolf, G. T., Fisher, S. G., and Carey, T. E. (2003) P53 mutation correlates with cisplatin sensitivity in head and neck squamous cell carcinoma lines. *Head Neck* **25,** 654–661
42. Andrews, G. A., Xi, S., Pomerantz, R. G., Lin, C. J., Gooding, W. E., Wentzel, A. L., Wu, L., Sidransky, D., and Grandis, J. R. (2004) Mutation of p53 in head and neck squamous cell carcinoma correlates with Bcl-2 expression and increased susceptibility to cisplatin-induced apoptosis. *Head Neck* **26,** 870–877
43. Cortés Sempere, M., Rodríguez Fanjul, V., Sánchez Pérez, I., and Perona, R. (2008) The role of the NFκB signalling pathway in cancer. *Clin. Transl. Oncol.* **10,** 143–147
44. Lin, Y., Bai, L., Chen, W., and Xu, S. (2010) (2010) The NF-κB activation pathways, emerging molecular targets for cancer prevention and therapy. *Expert Opin. Ther. Targets* **14,** 45–55
45. Grivennikov, S. I., and Karin, M. (2010) Inflammation and oncogenesis: a vicious connection. *Curr. Opin. Genet. Dev.* **20,** 65–71
46. Karin, M. (2009) NF-κB as a critical link between inflammation and cancer. *Cold Spring Harb. Perspect. Biol.* **1,** a000141
47. Kato, T., Duffey, D. C., Ondrey, F. G., Dong, G., Chen, Z., Cook, J. A., Mitchell, J. B., and Van Waes, C. (2000) Cisplatin and radiation sensitivity in human head and neck squamous carcinomas are independently modulated by glutathione and transcription factor NF-κB. *Head Neck* **22,** 748–759
48. Iliopoulos, D., Hirsch, H. A., and Struhl, K. (2009) An epigenetic switch involving NF-κB, Lin28, Let-7 MicroRNA, and IL6 links inflammation to cell transformation. *Cell* **139,** 693–706
49. Yang, J., Splittgerber, R., Yull, F. E., Kantrow, S., Ayers, G. D., Karin, M., and Richmond, A. (2010) Conditional ablation of Ikkb inhibits melanoma tumor development in mice. *J. Clin. Invest.* **120,** 2563–2574
50. Wang, D., Veena, M. S., Stevenson, K., Tang, C., Ho, B., Suh, J. D., Duarte, V. M., Faull, K. F., Mehta, K., Srivatsan, E. S., and Wang, M. B. (2008) Liposome encapsulated curcumin suppresses growth of HNSCC *in vitro* and in xenografts through the inhibition of NFκB by an AKT independent pathway. *Clin. Cancer Res.* **14,** 6228–6236
51. Cleveland, D. W., Yamanaka, K., and Bomont, P. (2009) Gigaxonin controls vimentin organization through a tubulin chaperone-independent pathway. *Hum. Mol. Genet.* **18,** 1384–1394
52. Urban, D., Corry, J., and Rischin, D. (2014) What is the best treatment for

patients with human papillomavirus-positive and -negative oropharyngeal cancer? *Cancer* **120,** 1462–1470
53. Kumar, B., Cordell, K. G., Lee, J. S., Worden, F. P., Prince, M. E., Tran, H. H., Wolf, G. T., Urba, S. G., Chepeha, D. B., Teknos, T. N., Eisbruch, A., Tsien, C. I., Taylor, J. M., D'Silva, N. J., Yang, K., Kurnit, D. M., Bauer, J. A., Bradford, C. R., and Carey, T. E. (2008) EGFR, p16, HPV titer, Bcl-xL and p53, sex, and smoking as indicators of response to therapy and survival in oropharyngeal cancer. *J. Clin. Oncol.* **26,** 3128–3137
54. Al-Swiahb, J. N., Huang, C. C., Fang, F. M., Chuang, H. C., Huang, H. Y., Luo, S. D., Chen, C. H., Chen, C. M., and Chien, C. Y. (2010) Prognostic impact of p16, p53, epidermal growth factor receptor, and human papillomavirus in oropharyngeal cancer in a betel nut-chewing area. *Arch. Otolaryngol. Head Neck Surg.* **136,** 502–508
55. Aderhold, C., Faber, A., Grobschmidt, G. M., Chakraborty, A., Bockmayer, A., Umbreit, C., Birk, R., Stern-Straeter, J., Hörmann, K., and Schultz, J. D. (2013) Small molecule-based chemotherapeutic approach in p16-positive and -negative HNSCC *in vitro*. *Anticancer Res.* **33,** 5385–5393
56. Lassen, P., Eriksen, J. G., Hamilton-Dutoit, S., Tramm, T., Alsner, J., Overgaard, J., and Danish Head and Neck Cancer Group (DAHANCA) (2010) HPV-associated p16-expression and response to hypoxic modification of radiotherapy in head and neck cancer. *Radiother. Oncol.* **94,** 30–35
57. Capece, D., Fischietti, M., Verzella, D., Gaggiano, A., Cicciarelli, G., Tessitore, A., Zazzeroni, F., Alesse E. (2013) The inflammatory microenvironment in hepatocellular carcinoma: a pivotal role for tumor-associated macrophages. *Biomed Res. Int.* **2013,** 187204
58. Chang, C. P., Su, Y. C., Lee, P. H., and Lei, H. Y. (2013) Targeting NFκB by autophagy to polarize hepatoma-associated macrophage differentiation. *Autophagy* **9,** 619–621
59. Cohen, A., Veena, M. S., Srivatsan, E. S., and Wang, M. B. (2009) Curcumin suppresses IL-6 and IL-8 production in head and neck cancer cells via inhibition of IkB kinase (IKK). *Arch. Otolaryngol. Head Neck Surg.* **135,** 190–197